

EXPERIMENTAL STUDY OF SPRAY COOLING OF ELECTRONICS OVER HIGH
HEAT FLUXED SURFACE

A THESIS SUBMITTED TO
THE GRADUATE SCHOOL OF NATURAL AND APPLIED SCIENCES
OF
MIDDLE EAST TECHNICAL UNIVERSITY

BY

ÇAĞRI BALIKCI

IN PARTIAL FULFILLMENT OF THE REQUIREMENTS
FOR
THE DEGREE OF MASTER OF SCIENCE
IN
MECHANICAL ENGINEERING

AUGUST 2013

Approval of the thesis:

**EXPERIMENTAL STUDY OF SPRAY COOLING OF ELECTRONICS OVER HIGH
HEAT FLUXED SURFACE**

submitted by **ÇAĞRI BALIKCI** in partial fulfillment of the requirements for the degree of
**Master of Science in Mechanical Engineering Department, Middle East Technical Uni-
versity** by,

Prof. Dr. Canan Özgen
Dean, Graduate School of **Natural and Applied Sciences**

Prof. Dr. Süha Oral
Head of Department, **Mechanical Engineering**

Dr. Tahsin A. Çetinkaya
Supervisor, **Mechanical Engineering Dept., METU**

Examining Committee Members:

Assoc. Prof. Dr. İlker Tari
Mechanical Engineering Department, METU

Dr. Tahsin A. Çetinkaya
Mechanical Engineering Department, METU

Assist. Prof. Dr. Metin Yavuz
Mechanical Engineering Department, METU

Dr. Özgür Bayer
Mechanical Engineering Department, METU

M.Sc. Uğur Alakoç
Senior Expert Thermal Engineer, ASELSAN-REHİS

Date:

28.08.2013

I hereby declare that all information in this document has been obtained and presented in accordance with academic rules and ethical conduct. I also declare that, as required by these rules and conduct, I have fully cited and referenced all material and results that are not original to this work.

Name, Last Name: ÇAĞRI BALIKCI

Signature :

ABSTRACT

EXPERIMENTAL STUDY OF SPRAY COOLING OF ELECTRONICS OVER HIGH HEAT FLUXED SURFACE

BALIKCI, ÇAĞRI

M.S., Department of Mechanical Engineering

Supervisor : Dr. Tahsin A. Çetinkaya

August 2013, 73 pages

Due to need for more powerful and rapider electron transformation requirements, electronic packages are getting denser. Unluckily, capability of transferring more electrons is also increased. As a result, especially recent semiconductor packages suffer from high heat fluxes, which can cause performance degradation and even burnt chips. For all of those reasons, an efficient and low thermal resistant heat transfer regime has to be applied onto those electronic components. Spray cooling for electronics is one of the best cures for this type of problems. Spray cooling utilizes latent heat of vaporization and pulverization of fluid particles so that large amount of heat can be rejected almost at constant temperature with small flow rates. In this study factors that affecting spray cooling for electronics performance, such as inclination angle, fluid type, mass flow rate and pressure difference, will be investigated by experimentally by using commercial dielectric fluids. At the end of the study, results will be compared with similar studies and empirical models.

Keywords: Electronics cooling, Breakup of fluids, Spraying, Dielectric fluid, Two-Phase heat transfer

ÖZ

YÜKSEK ISI AKISINA SAHİP ELEKTRONİK PARÇALARIN YÜZEYLERİNDE SPREY SOĞUTMA TEKNİĞİ ÜZERİNE DENEYSEL ÇALIŞMALAR

BALIKCI, ÇAĞRI

Yüksek Lisans, Makina Mühendisliği Bölümü

Tez Yöneticisi : Dr. Tahsin A. Çetinkaya

Ağustos 2013 , 73 sayfa

Elektronların daha hızlı ve daha güçlü taşınma ihtiyacı, elektronik parçaların daha yoğun bir şekilde paketlenmesine yol açıyor. Daha yoğun paketlenen elektroniklerin, ne yazık ki, güçleri de aynı şekilde artıyor. Bu uygulamaların sonucunda özellikle son zamanlarda geliştirilen yarıiletken teknolojisine ait parçalar performans kaybına ve hatta yanmış çiplere yol açan yüksek ısı akısından dolayı sorun yaşıyorlar. Tüm bu sebepler için bu elektronik parçaların üzerine düşük ısı dirence ve yüksek ısı transferi verimine sahip bir ısı transferi yöntemini uygulamak elzemdir. Sprey soğutma bu tip sorunlar için en iyi çözümlerden biridir. Sprey soğutma maddelerin faz enerjisinden yararlanarak yüksek miktarda ısı transferini mümkün kılarken, diğer bir yandan da akışkanları parçalarına ayırarak daha verimli bir ısı transferine yol açar. Bu çalışmada, elektronik parçaların soğutulmasına yönelik olan sprej soğutmanın performansının sprej açısıyla, akışkan tipiyle, kütle akısıyla ve basınçla nasıl değiştiğine dair ticari olarak satılan dielektrik sıvılar kullanılarak deneysel çalışmalar yapılacaktır. Çalışmalar sonucunda çıkan sonuçlar benzer çalışmalarla ve deneysel modellerle karşılaştırılacaktır.

Anahtar Kelimeler: Elektronik soğutma, Akışkanların parçalanması, Sprej, Dielektrik sıvı,
İki fazlı ısı transferi

to my Ancestors...

ACKNOWLEDGMENTS

First of all, I wish to express my deepest thanksgiving to my supervisor Dr. Tahsin A. etinkaya for his valuable critics, excellent supervision and endless support.

I would like to thank ASELSAN Inc. for facilities provided for the completion of this thesis.

I would also like to thank TBİTAK-BİDEB for their financial support during my graduate education.

I would like to express my all appreciation to Damla Erayta for her great patience and encouragements. I hope she keeps her support to me for all our life. This study cannot be completed without her. My family, Hasan Balıkcı, Reide Balıkcı and Aybike Balıkcı, are always behind me at this period, too.

At the end, I would to declare my graces about my colleagues. Ahmet Kırılılar, Hakan Boran, Necip ahan, Hakan Korkmaz, Vahdettin Ta, Uur Alako, Seluk ksz, Mustafa Dindar, Abdlkadir Ko and Alper Seren have never hidied their assistance to my work. They have always shown great care for completing my studies.

TABLE OF CONTENTS

ABSTRACT	v
ÖZ	vi
ACKNOWLEDGMENTS	viii
TABLE OF CONTENTS	ix
LIST OF TABLES	xi
LIST OF FIGURES	xii
LIST OF ABBREVIATIONS	xvi
CHAPTERS	
1 INTRODUCTION	1
1.1 Motivation of the Study	1
1.2 Objective of the Study	3
2 THEORY OF SPRAY COOLING AND LITERATURE REVIEW	7
2.1 Fluid Breakup Mechanism	7
2.2 Atomizer Types	12
2.3 Two Phase Heat Transfer	18
2.4 Literature Review of Spray Cooling Applications	23
3 EXPERIMENTAL SETUP AND PROCEDURE	31
3.1 Designing of a Spray Cooling Experimental Setup	31

3.2	Experimental Procedure	39
4	EXPERIMENT RESULTS	45
4.1	FC-72 Results	45
4.2	FC-84 Results	50
4.3	Heat Loss Calculation	55
4.4	Repeatability and Uncertainty of System	56
5	DISCUSSION AND CONCLUSION	59
5.1	Discussion on Experimental Results	61
5.2	Comparison of Experimental Results with Volumetric Flux Model (VFM)	62
5.3	Conclusion	64
5.4	Future Work	64
	REFERENCES	67
	APPENDICES	
A	DERIVATION OF VFM	71

LIST OF TABLES

TABLES

Table 2.1	Breakup Regimes [6, 7]	9
Table 2.2	Properties of Various Atomizers	15
Table 2.3	Numbers Driving Boiling and Condensation	19
Table 3.1	Fluid Properties at 25°C and 1 ATM	41
Table 3.2	Air Properties at 25°C and 1 ATM	41
Table 3.3	Other Properties of the System	41
Table 4.1	Dimensionless Numbers for FC-72 Experiments	45
Table 4.2	Breakup and Contact Regimes for FC-72 Experiments	45
Table 4.3	Dimensionless Numbers for FC-84 Experiments	50
Table 4.4	Breakup and Contact Regimes for FC-84 Experiments	50
Table 4.5	Two Same Experiments at $Q = 6.87 \times 10^{-6} \text{ m}^3/\text{s}$ by Using FC-72 at 0°	57
Table 4.6	Average Percentage Repeatability for Heat Flux and Temperature Measurements	57
Table 5.1	Comparison of Experimental and Empirical Spraying CHF for FC-72	63
Table 5.2	Comparison of Experimental and Empirical Spraying CHF for FC-84	63

LIST OF FIGURES

FIGURES

Figure 1.1 (a) First computer “ENIAC” [1] (b) Commodore64 [2] (c) A ultrabook [3]	1
Figure 1.2 Cost of manufacturing versus number of integrated components by year [4]	2
Figure 1.3 A burnt chip due to heat flux [5]	3
Figure 2.1 Breakup forces	8
Figure 2.2 Depiction of breakup regimes [7]	9
Figure 2.3 Droplet impact characteristics at different liquid We number [8] (a) Full rebound $We_l \leq 15 \pm 5$; (b) Rebound with breakup $20 \pm 5 < We_l \leq 50 \pm 5$; (c) Splashing limit $We_l \cong 60 \pm 10$; (d) Typical splashing region $60 \pm 10 < We_l \leq 350 \pm 20$; (e) Prompt Splash $We_l > 350$;	11
Figure 2.4 Atomizers from daily life	12
Figure 2.5 Atomizer types (a) Pressure jet atomizer (b) Two-fluid atomizer (c) Rotary atomizer	13
Figure 2.6 ATLAS toroid magnet (Courtesy of IRFU)	18
Figure 2.7 Boiling curve	20
Figure 2.8 (a) Transition boiling (b) Film boiling	22
Figure 2.9 An example for spray cooling experimental setup [18]	23
Figure 2.10 A well insulated sprayed surface [20]	24

Figure 2.11 Adjustable angle mechanism for a spray cooling setup [21]	25
Figure 2.12 Cooling of hybrid vehicle power electronics by (a) modifying existing R134a air-conditioning refrigeration loop and (b) using a separate cooling loop with ap- propriate coolant [25].	26
Figure 2.13 TIR (Total internal reflectance) technique [26].	27
Figure 2.14 Velocity vectors of a single droplet through a CFD analysis [27].	27
Figure 2.15 Impact history of a water droplet for fixed $We_l = 20$ [28].	28
Figure 2.16 Different shapes of enhanced surfaces [10].	28
Figure 2.17 Angle and chf relation [29].	29
Figure 3.1 Overview of experimental setup	32
Figure 3.2 Spray cooling loop	33
Figure 3.3 Manufacturing of spraying chamber	34
Figure 3.4 (a) 0° nozzle holder (b) 15° nozzle holder (c) 35° nozzle holder (d) 55° nozzle holder	35
Figure 3.5 Designing spray holders	35
Figure 3.6 Detailed view of spraying chamber	36
Figure 3.7 (a) Pressure dial gage (b) Electrically resistive pressure and temperature transducer (c) Mass flow meter	38
Figure 3.8 (a) Fan supply (b) Pump supply (c) Heat load supply	38
Figure 3.9 Flowchart of the experiment	39
Figure 3.10 Transient raw data from data logger	40
Figure 3.11 Transient reservoir tempearture and nozzle inlet pressure	40
Figure 4.1 0° boiling curve at different Q for FC-72	46

Figure 4.2	15° boiling curve at different Q for FC-72	46
Figure 4.3	35° boiling curve at different Q for FC-72	47
Figure 4.4	55° boiling curve at different Q for FC-72	47
Figure 4.5	Boiling curves at different angles at $Q = 3.77 \times 10^{-6} \text{m}^3/\text{s}$ for FC-72 . . .	48
Figure 4.6	Boiling curves at different angles at $Q = 6.87 \times 10^{-6} \text{m}^3/\text{s}$ for FC-72 . . .	48
Figure 4.7	Boiling curves at different angles at $Q = 9.17 \times 10^{-6} \text{m}^3/\text{s}$ for FC-72 . . .	49
Figure 4.8	Spraying CHF values at different angles for FC-72	49
Figure 4.9	0° boiling curve at different Q for FC-84	51
Figure 4.10	15° boiling curve at different Q for FC-84	51
Figure 4.11	35° boiling curve at different Q for FC-84	52
Figure 4.12	55° boiling curve at different Q for FC-84	52
Figure 4.13	Boiling curves at different angles at $Q = 3.68 \times 10^{-6} \text{m}^3/\text{s}$ for FC-84 . . .	53
Figure 4.14	Boiling curves at different angles at $Q = 6.72 \times 10^{-6} \text{m}^3/\text{s}$ for FC-84 . . .	53
Figure 4.15	Boiling curves at different angles at $Q = 9.28 \times 10^{-6} \text{m}^3/\text{s}$ for FC-84 . . .	54
Figure 4.16	Spraying CHF values at different angles for FC-84	54
Figure 4.17	Thermal camera image from spraying chamber	55
Figure 4.18	Cylindrical insulation jacket thermal image	56
Figure 5.1	First design of experiment setup	60
Figure 5.2	Last design of experiment setup	60
Figure 5.3	VFM and experimental results comparison for FC-72	62
Figure 5.4	VFM and experimental results comparison for FC-84	63
Figure A.1	Nomenclature for inclined spray	71

Figure A.2 Differential area ratio with respect to inclination angle, dA'/dA 72

LIST OF ABBREVIATIONS

A	Area
Bo	Bond Number
CHF	Critical Heat Flux
C_p	Specific heat
$C_{p,f}$	Specific heat of liquid
d	Diameter
d_0	Spray Orifice Diameter
d_{32}	Sauter Mean Diameter (SMD)
FCB	Free Convection Boiling
g	Gravity of acceleration
Gr	Grashof Number
h	Convection coefficient
h_{fg}	Latent Heat of Vaporization
H	Distance from orifice to projected surface
H_n	Distance from orifice to test surface
Ja	Jakob Number
k	Thermal conductivity
L	Characteristic length, test surface length
M	Measurement
NB	Nucleate Boiling
Nu	Nusselt Number
Oh	Ohnesorge Number
ΔP	Pressure Difference
Pr	Prandtl Number
q	Heat
q_r	Heat in radial direction
q''	Heat Flux
q''_{max}	Maximum Heat Transferred (CHF)
$q''_{s,CHF}$	Spraying CHF
$q''_{sub,max}$	CHF with Subcooling effect
Q	Flow rate
\bar{Q}	Average flow rate

\overline{Q}''	Average flow rate flux
r	Radius
r_1	Inner radius
r_2	Outer radius
R	Percentage repeatability
\overline{R}	Average percentage repeatability
\overline{R}_q	Average percentage repeatability for heat flux measurement
\overline{R}_T	Average percentage repeatability for temperature measurement
Re	Reynolds Number
Re_l	Liquid Reynolds Number
T	Temperature
T_s	Surface temperature
$T_{s,1}$	Inner surface temperature
$T_{s,2}$	Outer surface temperature
T_{in}	Inlet temperature
T_{sat}	Saturation temperature
ΔT_{sub}	Subcooling temperature
ΔT_e	Excess temperature
TB	Transition Boiling
U	Velocity
We	Weber Number
We_a	Air Weber Number
We_l	Liquid Weber Number
We_{d_0}	Spray Weber Number
α	Inclination angle of test surface from normal
μ	Absolute viscosity
μ_f	Absolute viscosity of liquid
ρ	Density
ρ_l	Liquid density
ρ_f	Liquid density
ρ_g	Gas density
ρ_v	Vapor density
ρ_a	Air density
σ	Surface tension
σ_f	Liquid surface tension
θ	Spray cone angle

CHAPTER 1

INTRODUCTION

1.1 Motivation of the Study

Technology never stops improving. People are always highly passionate demanders who are looking for the ways to defeat nature. Therefore, it is not hard to say that there has been a constantly growing improvement curve of civilization since Paleolithic ages to modern times. However, the interesting side of this statement is that current era is the best example for observation of development so; humanity has never been greedy for the best as much as today.

“The bloom of technology” in this era contains millions of sample. Every appliance in our living room, in our military or in our hospital has a more recent version produced in just a few days. Computers, for example, are the best examples of how fast everything has changed.

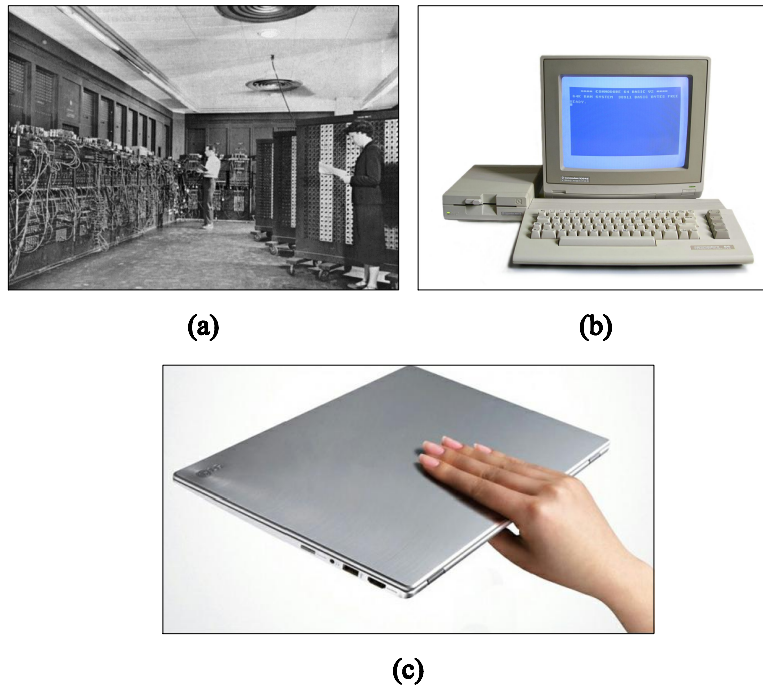


Figure 1.1: (a) First computer “ENIAC” [1] (b) Commodore64 [2] (c) A ultrabook [3]

A large room was required to make 5000 calculations in a second at the mid of 20th century. It was aimed to run meteorological calculations at huge supercomputers for forecasting. By starting 1980s, technology was first used to make fun in our home. A gigantic supercomputer of 1950s was contracted behind a 13" glass for computerization of every family. Nowadays, a computer can be hold at palm of hand is able to solve a highly loaded aerodynamic transient analysis in just a couple of hours. As a consequence, desire for mobility of technology is never behind the desire for power.

Semiconductor technology is the locomotive power of electronic industry, which has been firstly introduced in last quarter of 1950s. After offering semiconductor technology, it is possible to intensify the power of electrons into very small areas. This was a monumental step for humanity since; mankind landing to the Moon has been possible after integrating semiconductors into vehicles. The interesting fact of this phenomenon is that today's a simple mobile phone is far more powerful than its ancestor placed in "Apollo 11".

Gordon Moore, one of the founders of Intel Corporation, is very famous with "Moore's Law". He basically states that more transistors will be placed into more small areas year by year. Additionally, the cost of production will decrease [4]

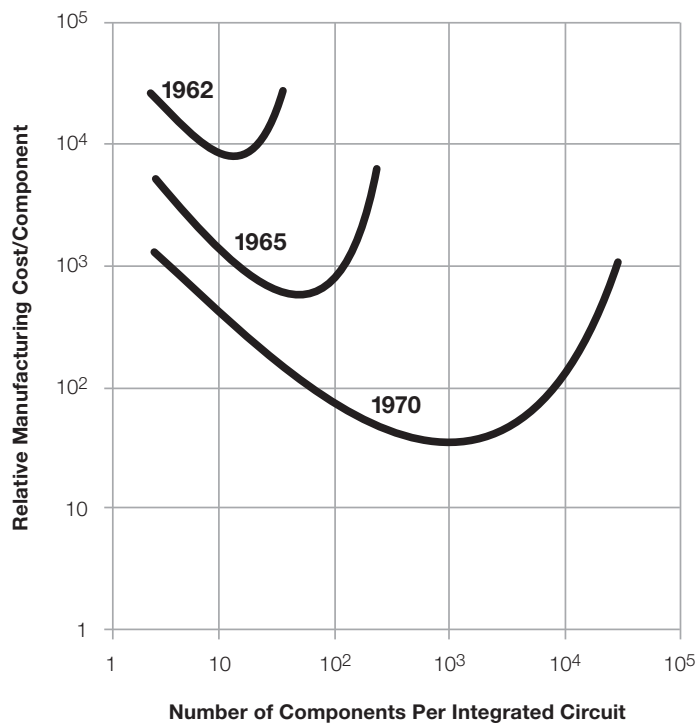


Figure 1.2: Cost of manufacturing versus number of integrated components by year [4]

Figure 1.2 draws the future of electronics industry. This is the original curve drawn by Moore in the year of 1965.

Until this point, motivation of this study hides behind electronic industry. Mechanical engineering side of this study is rather complicated and striking.

Dissipated heat is one of the important problems of the nature. Any of the systems, from complicated one to basic assemblies, do not hold 100% efficiency. It is impossible and every thermodynamic book underlines this fact at the very start. Therefore, it is expected that miniature semiconductor assemblies suffer from high rate of heat dissipation. As a result, their reliability and operational capability are limited by how much heat can be rejected from the system within safe temperature gradients.

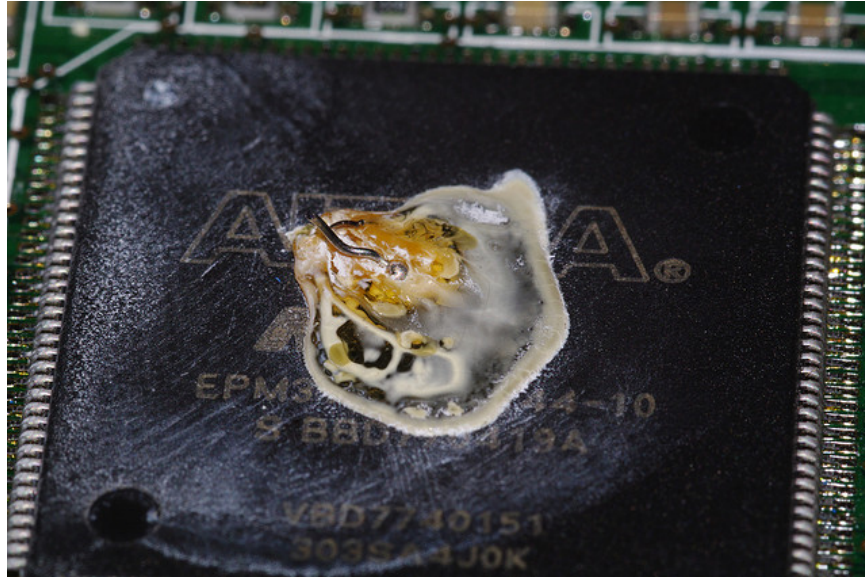


Figure 1.3: A burnt chip due to heat flux [5]

Consequently, electronics are far denser and more powerful today when compared to ones at mid of the 20th century. Dense packages create high heat loads at very narrow areas. Thus, high heat fluxes occur and may possibly damage assemblies. Motivation of this study is applying a specialized cooling technique to rapidly growing electronic industry so that components can reach their maximum power limits with maximum reliability.

1.2 Objective of the Study

Obtaining an effective and utilizable heat transfer solution for highly dense and microelectronic packages is not just choosing a technique and applying. Lots of engineering parameters have to be considered before integrating a thermal design into an electronic system. Cost, performance, sustainability, reliability, applicability etc. are basic criteria that have to be considered at the very start of system design.

Nature of matter offers variety of heat transfer scheme for cooling down electronics. Nevertheless, requirements ought to be well pointed for accomplish the motivation of this study.

As a reminder, it has to be underlined that electronic packages built over semiconductor technology are very susceptible to high thermal gradients. Their performances can be sharply

degraded because of high thermal resistance.

The first task for a thermal design engineer creating a cooling system for electronic packages is deciding whether it will be a single-phase system or two-phase system. Both of them has advantages and disadvantages as expected. A single phase heat transfer is advantageous since; complexity of components and system is not at high level. Supplying a pressure gradient on a system is enough mostly. Cooling an electronic system with fans is the basic approach for single phase system.

Although so many problems can be solved with single phase approach, single phase heat transfer carries a critical point. It is almost impossible to keep the medium temperature constant when applying single phase heat transfer scheme. On the other hand, two-phase heat transfer makes possible to remove large amount of heat compared to single phase heat transfer at almost constant temperature. Unfortunately, system complexity and component number can increase. Therefore, it would not be a wrong statement that two-phase heat transfer is a suitable solution for high heat dissipaters.

Two-phase heat transfer has lots of application areas; even a refrigerator in a kitchen takes advantage of latent heat of vaporization. Nonetheless, they are built in different approaches. For example, two-phase heat transfer can be applied on a still liquid whereas; a highly pressurized oil jet is a good solution for quenching steel bars. However, if the problem is based on an electronic system, there are bunch of constraints:

- The cooling medium and electronic assemblies must not interact with each other. For that reason, special liquids, named as dielectric fluids, are preferred. They have almost no effect on electronic systems so; they can be used safely. Unluckily, they have low thermal conductivities when compared to water.
- Most of the semiconducting electronic packages cannot survive when their case temperatures exceed $100^{\circ}C$. Therefore boiling point of the liquid has to be selected with great attention.
- Electronic packages are not strong packages in structural meaning so that applying high pressurized liquid or gas onto their surface can damage them.

Behind those limitations above, consider the general heat conduction equation:

$$\nabla T = -\frac{q}{kA} \quad (1.1)$$

The ideal case for a perfect conductive system temperature gradient is zero. In other words, no matter how much heat is dissipated, sink and source temperature will be the same. This is the main aim of a thermal system for the best performance. This is impossible, of course. For

that reason either thermal conductivity k or heat surface area A or both has to be maximized for low resistance system.

$$\lim_{\substack{k \rightarrow \infty \\ A \rightarrow \infty}} \nabla T = 0 \quad (1.2)$$

The challenging side of a thermal system design is increasing those parameters. k is material dependent property so that it is not easy to increase it. Additionally, there are probably other parameters that are not possible to be given out just for conductivity. As a result, design side has to consider the ways for increasing heat transfer area.

This is the point where the “Spray Cooling” answer blinks. Spray cooling carries all of the superior characteristics of electronics cooling. Firstly, fluid stream can be dispersed into finer particles by using a spraying nozzle so; heat transfer area is increased. Spray cooling for electronics technique use special fluids made from fluorochemicals. These fluids have relatively low boiling points when compared to water. Therefore, a system can use the advantage of latent heat of vaporization by using those fluids. Besides, they are sold commercially in their dielectric form.

The objective of this study is examining spray cooling technique for electronics cooling by using dielectric fluids. However, experiment scheme cover different parameters. First, geometric parameters are changed. The angle of nozzle will be varied for determining how spraying performance is changing with different angle of spray. Secondly, pressure supplied to the system will be altered for finding the effects of different rate of pressure supply on heat transfer performance. Fluid type is another input to the experiment. At the end of the experiments, different boiling curves for different angles, fluids and pressures will be had. Moreover, results will be compared with some empirical models in literature.

CHAPTER 2

THEORY OF SPRAY COOLING AND LITERATURE REVIEW

Spray cooling is an interdisciplinary application for that reason; it is needed to mention lots of subject to getting familiar with it. It is a coupled operation that covering both fluid mechanics and heat transfer areas. The first action of spraying mechanism is dividing large fluid particles into finer particles. This is called as “Break-up mechanism”. This operation is carried out with special instruments known as “Atomizers”. After having completed fluid mechanics side, heat transfer is started when droplets intrude into heat transfer zone. For spray cooling action heat transfer is in “Boiling regime” or it can be named as “Two-phase heat transfer”. All in all, those complete processes above hold huge knowledge cluster in literature.

In this chapter, all of those will be investigated. The outline of this chapter is in the following row:

1. Fluid Break-Up Mechanism
2. Atomizer Types
3. Two Phase Heat Transfer
4. Literature Review of Spray Cooling Applications

2.1 Fluid Breakup Mechanism

Fluid breakup is, basically, making smaller fluid particles by means of applying forces on larger fluid particles. It can be also said that breakup is defeating the forces trying to hold fluid particles into the same form. These forces are originated from viscosity and surface tension of fluid.

In a breakup process, surface tension plays a crucial role that a liquid droplet will stay in a spherical form unless surface tension is exceeded. For instance, it can be observed that a drop of mercury at room temperature has a very high tendency to stay in a spherical shape. If it is distorted by a stick it will be scattered into the smaller particles. This is just because of overcoming the surface tension.

Viscosity causes another resistance for breakup mechanism. It has the same effects with surface tension just resisting to disintegration of fluid particles by means of shear stress.

Forces that cause breakup can be described in such a scheme:

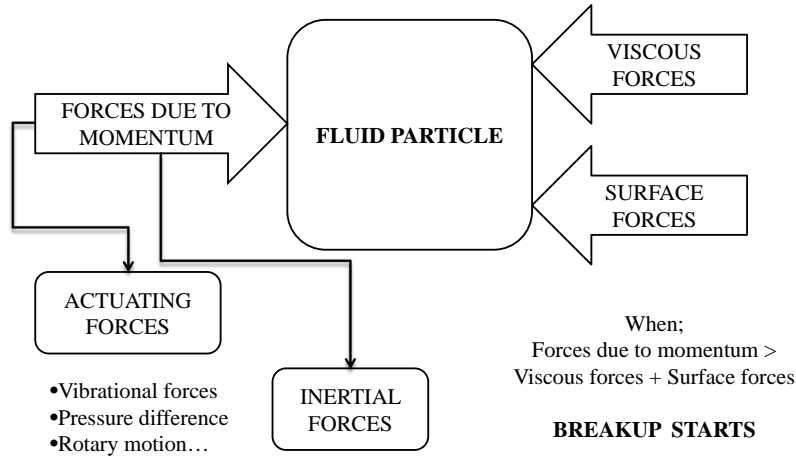


Figure 2.1: Breakup forces

Breakup is nothing but winning over the viscous and surface forces. Therefore, it will be very meaningful to mention *Reynolds Number* and *Weber Number* which are the definitions of ratio of inertial forces to viscous forces and inertial forces to surface tension forces, respectively.

$$Re = \frac{\text{InertialForces}}{\text{ViscousForces}} = \frac{\rho U L}{\mu} \quad (2.1)$$

$$We = \frac{\text{InertialForces}}{\text{SurfaceTensionForces}} = \frac{\rho U^2 L}{\sigma} \quad (2.2)$$

Another dimensionless number is obtained by using *Re* and *We* number. This number is called as *Ohnesorge Number*. *Oh* number is recognized in different ways in literature such as: stability number, viscous group or ratio of viscosity forces to surface tension forces.

$$Z = Oh = We^{0.5} Re^{-1} = \frac{\mu}{(\rho \sigma L)^{0.5}} \quad (2.3)$$

Ohnesorge has divided breakup types into four regimes by increasing velocity. These types are listed below [6, 7]:

1.Rayleigh Jet Breakup: Fluid particles break up due to the axisymmetric oscillations because of surface tension. Droplet diameter is larger than jet diameter.

2.First Wind-Induced Breakup: Surface tension effect is felt less than Rayleigh Jet Breakup since, the velocity difference between jet and air causes static shear force because of viscosity. Disintegration of fluid is rapider and droplet diameter is almost equal to the jet diameter.

3.Second Wind-Induced Breakup: Surface tension effect is nearly diminished because; increasing velocity makes dynamic pressure dominant. Unstable growth of short wavelength surface waves stir up breakup process. Droplet diameters are much less than the jet diameter.

4.Atomization: The jet breaks up totally and gets into a conical shape. Breakup occurs at a very short distance from exit port of fluid. The behaviour of flow is highly chaotic, irregular and unpredictable. The diameter of the droplet is very much smaller than jet diameter.

Table 2.1: Breakup Regimes [6, 7]

<i>Regime</i>	<i>Description</i>	<i>Predominant drop formation mechanism</i>	<i>Criteria for transition to next regime</i>
<i>1</i>	Rayleigh breakup	Surface tension force	$We_a > 0.4$ or; $We_a > 1.2 + 3.4Oh^{0.9}$
<i>2</i>	First wind-induced breakup	Surface tension force; dynamic pressure of ambient air	$1.2 + 3.41Oh^{0.9} < We_a < 13$
<i>3</i>	Second wind-induced breakup	Dynamic pressure of ambient air opposed by surface tension force initially	$13 < We_a < 40.3$
<i>4</i>	Atomization	Unknown	$We_a > 40.3$ or; $Oh \geq 100Re_l^{-0.92}$

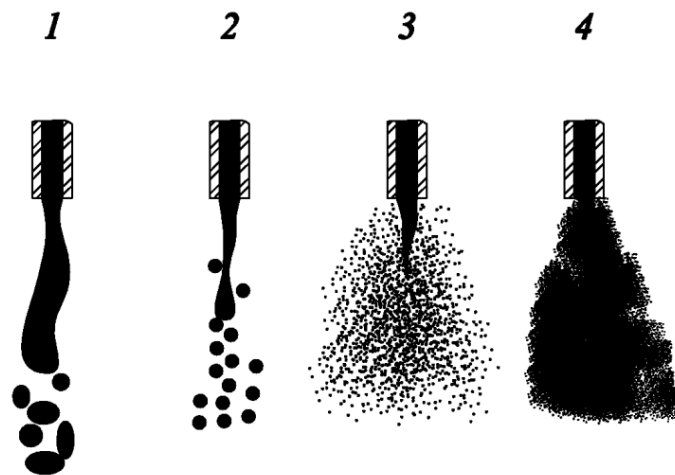


Figure 2.2: Depiction of breakup regimes [7]

Another issue with breakup process is that liquid coming out from orifice is not divided into the particles immediately. Breakup process always looks for a force balance unless droplets

fit into a stable shape. Therefore, enough departure time and enough distance from to surface are the key parameters when considering efficient dispersion.

Up to this point, breakup in free air is considered. Pressurized liquid leaves from the orifice, and it shows different behaviours according to Re , We and Oh numbers. However, there is, usually, a confined surface or another liquid that will contact with the atomized fluid in general spraying applications. This engagement of two mediums results in momentum transfer, which is also classified with flow parameters.

We_l is the main parameter determining the behavior of this momentum interchange [8]. Surface characteristics also regulate collision of drops and surface. These surface characteristics are:

1. *Surface temperature*
2. *Surface roughness*
3. *Surface patterns*

Firstly, temperature of the surface is a very important factor affecting the path of impinged drops. It is stated by Liu [7] that the temperature of the surface can predetermine whether the drops are splashed or rebounded. According to Liu, rebounding of droplets is less on a hot surface when compared to a cold surface. Nonetheless, hot-cold wall case is only important when considering transient problems or a single droplet. Wall temperature will settle down on a steady state temperature as operation continues. On the other hand, if intermittent operation is available, hot-cold wall case carries great importance.

Surface roughness is another attractive parameter to investigate. It is observed that droplets are more susceptible for being shattered when compared to polish surface. Additionally, the contact area between liquid and solid is increased by introducing rough surface [9]. One more step beyond the surface roughness is creating surface patterns for increasing extra surface areas. Silk et al. [10] produce different surface patterns for monitoring the effect of extended surfaces on spray cooling applications.

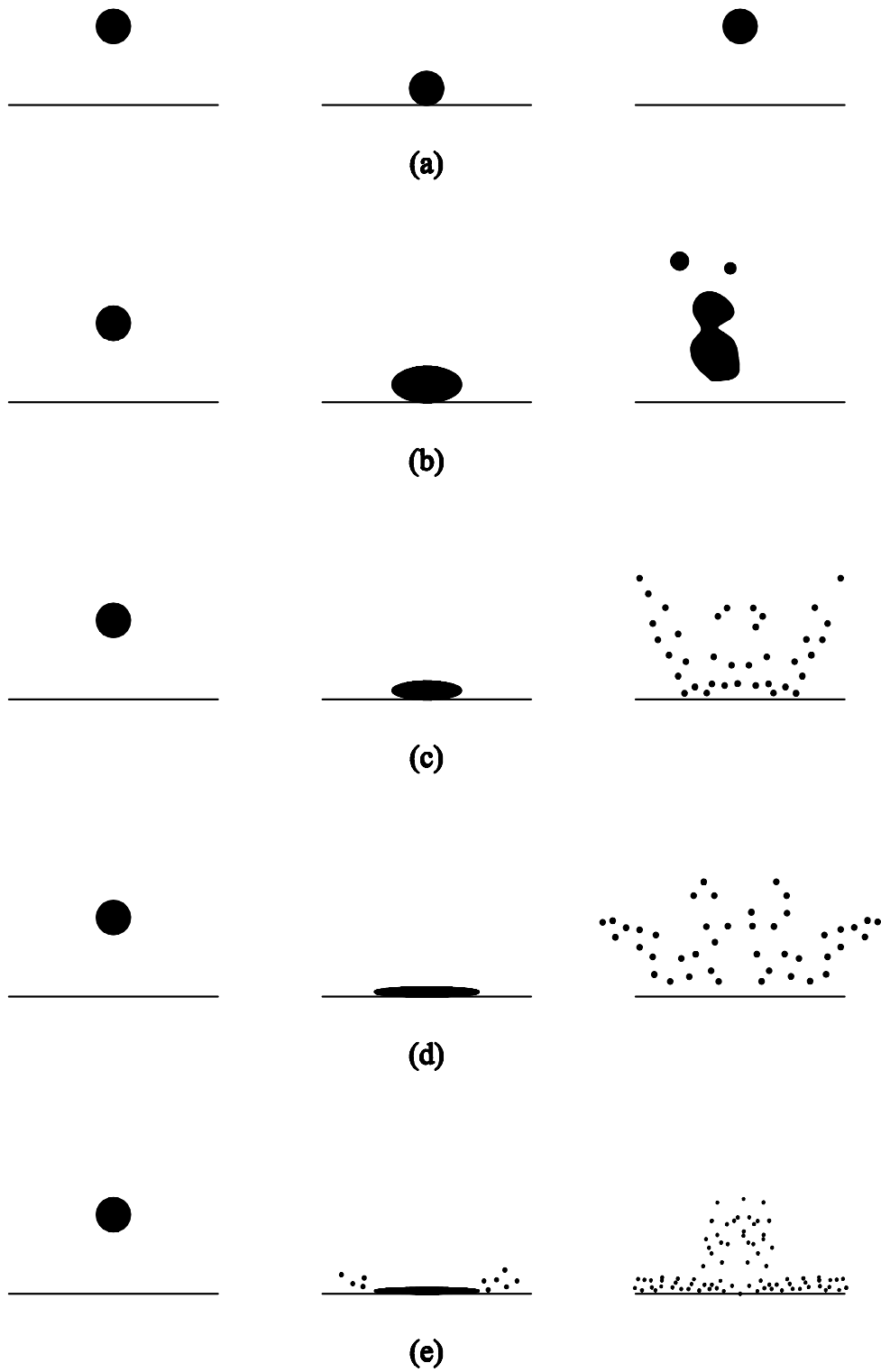


Figure 2.3: Droplet impact characteristics at different liquid We number [8] (a) Full rebound $We_l \leq 15 \pm 5$; (b) Rebound with breakup $20 \pm 5 < We_l \leq 50 \pm 5$; (c) Splashing limit $We_l \cong 60 \pm 10$; (d) Typical splashing region $60 \pm 10 < We_l \leq 350 \pm 20$; (e) Prompt Splash $We_l > 350$;

2.2 Atomizer Types

Atomizer is the most crucial element in a spraying system. It is basically a tool to transfer momentum on fluid particles. Fluid breakup process initiate by means of atomizers. Atomizers' main aim is creating fine droplets at atomization type breakup as it is interpreted by its name. After having channeled forces over the fluid particle, what is produced is called as *spray, mist, fog or aerosol*. Atomizers cover a wide area of usage even in daily life. A deodorant head or a bug spray is nothing but an atomizer placed on a pressure vessel. It utilizes the pressure embedded in the close vessel to produce mist.



Figure 2.4: Atomizers from daily life

In literature atomizer types are categorized according to mechanism that is preferred in it. Liu [7] and Bayvel and Orzechowski [11] have classified liquid atomizers into four categories. Those are:

1. *Pressure atomizers*
2. *Two-fluid atomizers*
3. *Rotary atomizers*
4. *Special atomizers*

Pressure atomizers are the most common atomizers used in engineering applications. In pressure atomization, pressure energy is converted to kinetic energy to accelerate fluid particles so that atomization can take place. Fundamental design of a pressure atomizer is not complex than an orifice, which employs the advantage of sudden area change.

Two-Fluid atomizers have great benefits when pressure atomization rate is not satisfactory. Two-fluid atomizers can sustain finer droplets under the same intake condition of mainstream liquid.

The essential difference of two-fluid atomizers is utilization of a pressurized gas for decomposition of liquid that is desired to be broken up. It is possible to have a better atomization

rates by two-fluid atomizers although, inlet pressure or mass flow rate is lower compared to a typical pressure atomizer case. However, this kind of atomization requires additional material supply, pressurized gas, which can cause additional cost on a spraying system. Additionally, more reliable and stronger materials ought to be chosen for more sustainable systems since, higher pressure rates are available.

Rotary atomizers occupy the centrifugal force for atomization. The most general method for rotary atomization is rotating cup in a chamber. A fluid is introduced into the area between rotating cup and chamber and then, it will be atomized by means of shear forces due to velocity gradient. Velocity of cup is increased to have a better rate of atomization. Rotary atomizers are usually preferred for agricultural applications such as, aerial fertilizing or pesticide dispersion on fields.

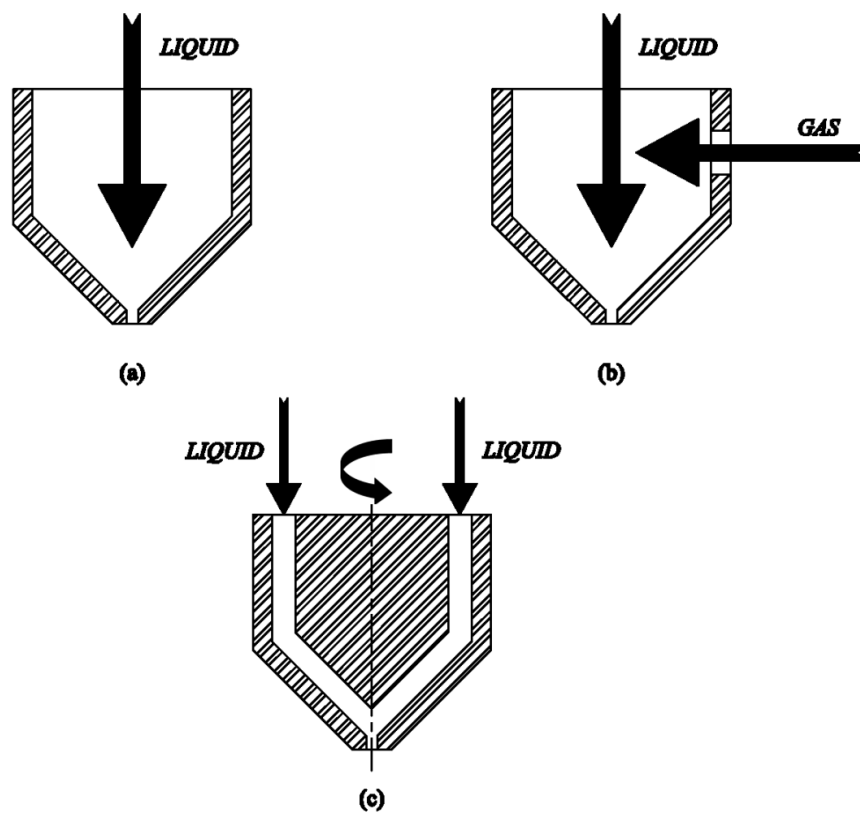


Figure 2.5: Atomizer types (a) Pressure jet atomizer (b) Two-fluid atomizer (c) Rotary atomizer

Special atomizers utilize different actuation mechanism rather than fluid or gas pressure. Outputs of this kind of atomizers are more controllable than conventional types. Atomization rate, frequency and even droplet size can be adjusted by direct controlling of special atomizers. Alas, they are more expensive, less reliable and in need of frequent maintenance.

Bayvel and Orzechowski [11] have named special atomizers according to actuation type such

as acoustic atomizers, ultrasonic atomizers, electrostatic atomizers and pulsary atomizers. Liu [7] has also added effervescent atomizers and whistle atomizers. Whistle atomizers are also known as acoustic or ultrasonic atomizers. Despite the fact that list contains of six types of special atomizers, new ones are added day by day.

Acoustic atomizers conduct acoustical energy to fluid through the waves. This type of atomizers operates in hearable frequency, 0.016-20 kHz. Nevertheless, acoustic atomizers are not able to produce fine sprays. Typical droplet size for a spray cooling application is about 25-200 μm . An acoustical atomizer has to operate at 50 MHz excitation frequency to create such sizes, though.

Ultrasonic atomizers have the same working principal with the acoustic atomizers. The only difference is that operation frequency of an ultrasonic atomizer is above 20 kHz, which is in ultrasonic band. This ability makes it possible to produce finer droplets than an acoustic atomizer. The disadvantageous sides of ultrasonic atomizers, however, are low flow rate and complexity and cost of ultrasonic wave generator. Complexity and cost disadvantage can be terminated by using piezoelectric material, which has outnumbered examples in recent studies.

Electrostatic atomizers are densely used in inkjet printers, so it is not hard to identify them as cutting edge for printing technologies. In an electrostatic atomizer, fluid particles are charged with electromagnetic forces so that surface tension forces and viscous forces can be defeated. Electrostatic atomization is favorable when droplets resist for drifting. Agricultural pesticide applications are another usage area for electrostatic atomizers. More coverage area is supplied by applying electrostatic forces to pesticides.

Pulsatory atomizers, on the other hand, do not offer a new atomization technique. Additional disturbances are added to conventional atomizers by pulsatory atomizers. To reach a neater definition, pulsatory atomizers are used for adding control mechanism on conventional atomizers, such as pressure atomizers, two fluid atomizers or rotary atomizers. This enhancement is usually carried out by a spring-load mechanism and maximum disturbance frequency is about 200 Hz. Therefore, it has to be expected that finer pulverization, such as atomization, cannot be attained just using pulsatory atomizers.

Effervescent atomizers are very special atomizers carry operation in combustion technologies. Oxygen and fuel are already mixed just exiting before orifice by using effervescent atomizers. It is similar to two-fluid atomizers but, difference is that main focus of effervescent atomizers are mixing of oxygen and fuel not scattering the fluid into fine particles by using gas kinetic energy.

Liu [7] has tabulated atomizer types under categories that are method, droplet size, application, advantage and disadvantage:

Table 2.2: Properties of Various Atomizers

<i>Method</i>	<i>Sub-method</i>	<i>Droplet Size</i> (μm)	<i>Application</i>	<i>Advantage</i>	<i>Disadvantage</i>
Pressure Atomization	Plain Orifice	20-250	Diesel engines, Jet engine afterburners, Ramjets	Simple, Rugged, Cheap	Narrow spray angle, Solid spray cone
	Simplex	20-200	Gas turbines, Industrial furnaces	Simple, Cheap, Wide spray angle	High supply pressure, Varying spray angle with pressure differential
	Dual Orifice	20-200	A variety of aircraft and industrial gas turbines	Good atomization, Turndown ratio 50:1, Relatively constant spray angle	Poor atomization in transition range, complexity in design, susceptibility of small passages to blockage
	Spill Return	20-200	A variety of combustors	Simple, Good atomization range over liquid flow rate, low risk of passage blockage	Varying spray angle with flow rate
	Fan Spray	100-1000	High pressure painting/coating, Annular combustors	Good atomization, Narrow elliptical spray pattern	Narrowing spray angle
	Duplex	20-200	Gas turbine combustors	Simple, Cheap	Narrowing spray angle with increasing liquid flow rate

Table 2.2: (Cont'd)

<i>Method</i>	<i>Sub-method</i>	<i>Droplet Size (μm)</i>	<i>Application</i>	<i>Advantage</i>	<i>Disadvantage</i>
Rotary Atomization	Spinning Disk	10-200	Spray drying, Aerial distribution of pesticides. Chemical processing	Good mono-dispersity of droplets. Independent control of atomization quality and flow rate	Satellite droplets, 360° spray pattern
	Rotary Cup	10-320	Spray drying, Spray cooling	Capable of handling slurries	Possible requirement for air blast around periphery
Two-Fluid Atomization Air-Assist	Internal Mixing	50-500	Industrial furnaces, Industrial gas turbines	Good atomization, low risk of blockage, suitable for high-viscosity fld.	Requirements for external source of high pressure gas
Two-Fluid Atomization Air-Assist	External Mixing	20-140	Industrial furnaces, Industrial gas turbines	Good atomization, low risk of blockage, suitable for high-viscosity fld.	Requirements for external source of high pressure gas
Two-Fluid Atomization Air-Blast	Plain-jet	15-130	Industrial gas turbines	Simple, cheap, good atomization	Narrow spray angle. Atomizing performance inferior to pre-filming air-blast type

Table 2.2: (Cont'd)

<i>Method</i>	<i>Sub-method</i>	<i>Droplet Size (μm)</i>	<i>Application</i>	<i>Advantage</i>	<i>Disadvantage</i>
	Pre-filming	25-140	Wide range of aircraft and industrial gas turbines	Good atomization especially at high ambient pressures. Wide spray angle	Poor atomization at low air velocities
Effervescent Atomization		20-340	Combustion	Simple, reliable, very good atomization, cheap, low risk of blockage. Easy maintenance.	Need for separate supply of atomizing air
Electrostatic Atomization		0.1-1000 300-600 100-250	Paint spraying, Printing, Oil burner	Fine and uniform droplets	Very low flow rates, strongly dependent on liquid electrical properties
Ultrasonic Atomization		1-5 30-60	Medical Spray, humidification, spray drying, acid etching, printing circuit, combustion	Very fine and uniform droplets, Low spray rates	Incapable of handling high liquid flow rates
Whistle Atomization		7-50	Atomization of liquid metals for powder production	Fine droplets, high gas efficiency	Broad droplet size distribution

Maintenance and sustaining long-term reliable operation of atomizers are important topics of spraying applications. Atomizers are sensitive devices no matter which type is chosen. Therefore, necessary actions have to be carefully taken when creating a new spraying system.

The first problem that is mostly encountered at atomizers is corrosion. If the material of atomizer and fluid used in application are not suitable to use together in terms of chemical stability, atomizer performance will degrade as operation continues. Investigation of chemical properties of substance that will be used in a spraying system is a must at the start of system design.

Blockage of orifice is another widely happening problem in atomizing systems. Intrusion of unintended particles cause blockage. Additionally, this problem can sometimes stem from corrosion because of material etched from surfaces. Therefore filtering is a very essential part of a spraying system. Filter passage size is selected such that it will be at least lower than 30% of orifice diameter. Nevertheless, the narrower the filter passage, the more pump power is required. Hence, this trade-off has to be adjusted so that a reliable operation and long term maintenance periods are possible.

Unlike conventional atomizers, pressure, two-fluid and rotary, the special atomizers have usually complex mechanisms into themselves. For that reason, if a case could be solved with a conventional atomizer, it would be a nice move not to use a special atomizer.

2.3 Two Phase Heat Transfer

Two-phase heat transfer is a very special mode of heat transfer since; it is possible to accumulate enormous heat with a little temperature increase. The nature has donated a great tool to engineers by offering phase change energy at almost constant temperature. People get benefit from latent heat of matter in many fields, from a complicated scientific problem to basic daily life appliances.

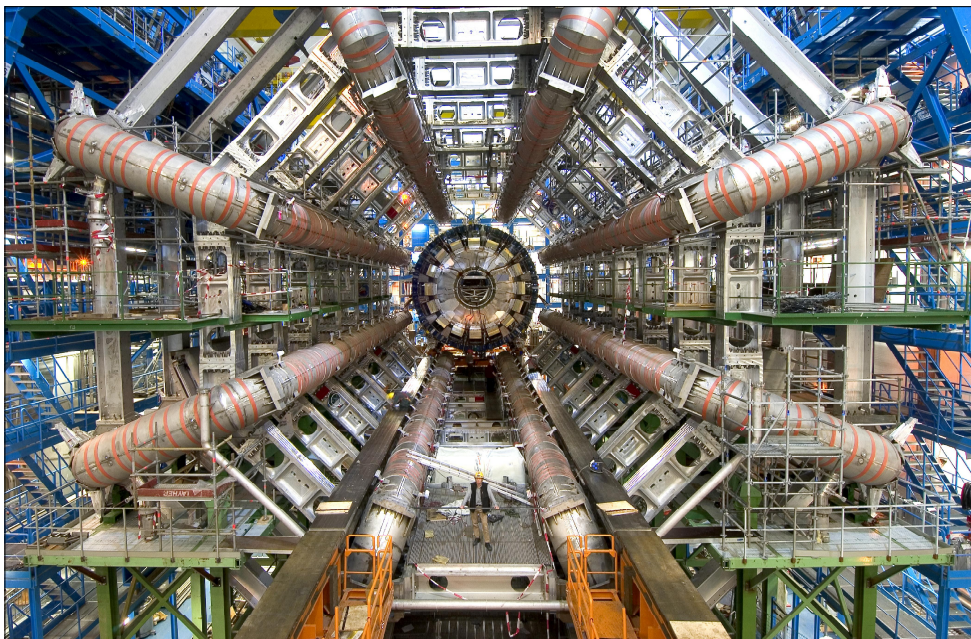


Figure 2.6: ATLAS toroid magnet (Courtesy of IRFU)

The ATLAS particle accelerator's magnets and toroids are cooled down by a huge refrigeration cycle. In the Atlas two separate helium refrigerators are placed to cool down 66 kW heat load [12]. Cooling system of the Atlas has to be superior because; it is aimed that temperature of magnets must stay near the absolute zero to ensure superconductivity for being able to accelerate particles. All in all, this is the supremacy of phase change in view of heat transfer.

Incropera et al. have investigated the dimensionless numbers drive boiling and condensation by Buckingham pi theorem [13]. There are 10 variables and 5 dimensions for defining heat transfer coefficient in two-phase heat transfer systems. According to Buckingham pi theorem $10 - 5 = 5$ dimensionless numbers are used for calculating heat transfer coefficient.

Table 2.3: Numbers Driving Boiling and Condensation

VARIABLES		PI-GROUPS	
$\frac{\Delta T_e}{T_{sat}} = T_s -$	ρ	$\frac{hL}{k}$	<i>Nusselt Number</i>
$g(\rho_l - \rho_v)$	C_p	$\frac{\rho g(\rho_l - \rho_v)L^3}{\mu^2}$	Buoyancy-viscosity ratio; likely <i>Grashof Number</i>
h_{fg}	k	$\frac{C_p \Delta T_{sub}}{h_{fg}}$	<i>Jakob Number</i>
σ	μ	$\frac{\mu C_p}{k}$	<i>Prandtl Number</i>
L	h	$\frac{g(\rho_l - \rho_v)L^2}{\sigma}$	<i>Bond Number</i>

The summary of the table is:

$$Nu = f \left[\frac{\rho g(\rho_l - \rho_v)L^3}{\mu^2}, Ja, Pr, Bo \right] \quad (2.4)$$

If the numbers are explained shortly: Nu depicts the ratio of convective heat transfer rate to conductive heat transfer rate in the boundary layer. The second number in Table 2.3 is very similar to Gr which is used excessively in natural convection problems. Gr is basically ratio of buoyancy forces to viscous forces in boundary layer. Ja is the ratio of sensible heat transfer rate to latent heat transfer rate. Ja is usually a small number for the reason that phase change energy is far larger than sensible energy. Bo is the ratio of buoyancy forces to surface tension forces.

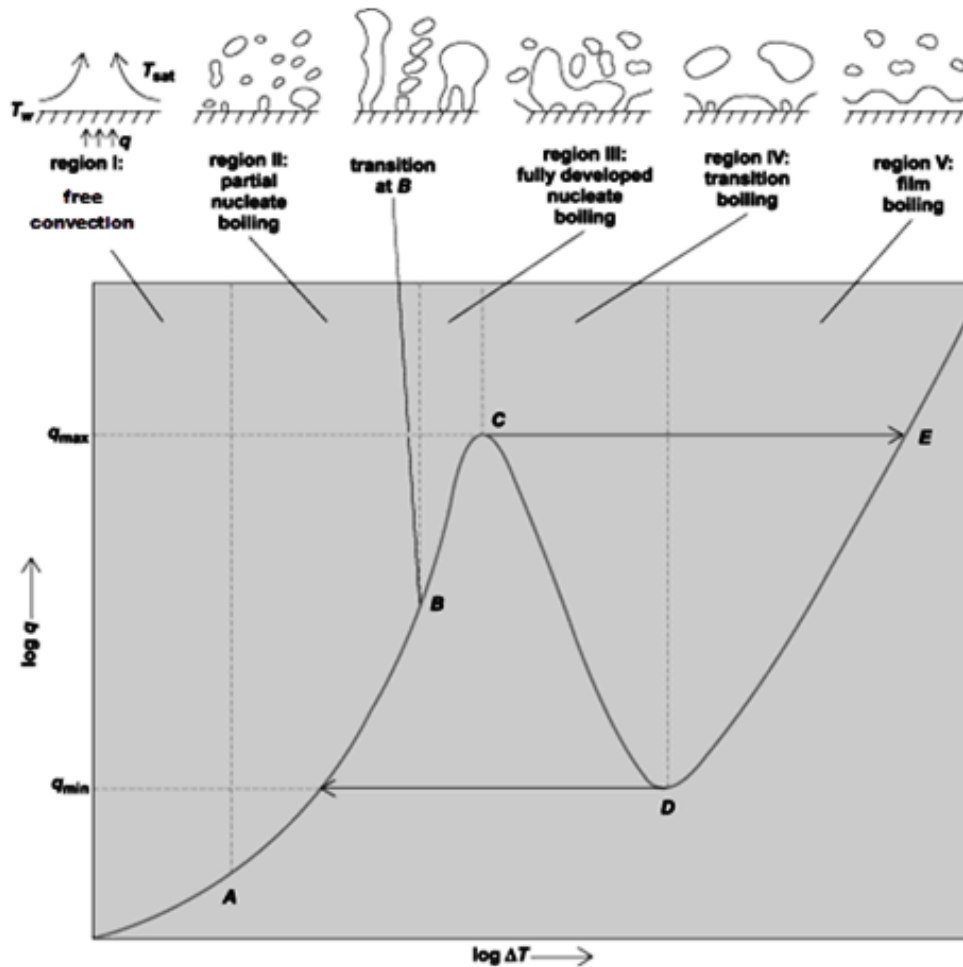


Figure 2.7: Boiling curve

Figure 2.7 is a very famous curve in the field of two-phase heat transfer. It was first discovered and stated by famous Japanese scientist, Nukiyama. Nukiyama designed an experiment setup for observing the boiling phenomena more precisely [14]. Nukiyama placed a platinum wire in a water bath at atmospheric pressure. The platinum wire was planned to be heated up by heat-fluxed controlled method. Then, temperature of the wire and heat flux supplied to the wire are measured.

Nukiyama subcategorized boiling into the four regimes:

- Free convection boiling
- Nucleate boiling
- Transition boiling
- Film boiling

All of them have different quantitative and visual characteristics. Some of them can be ob-

served with naked eyes, however for very high temperature, such as $1000\text{ }^{\circ}\text{C}$, there would be need of special equipments. Besides, boiling with different temperature difference has a hysteresis effect and Nukiyama stated that this was the result of power-controlled experiment approach.

The first mode of the boiling is named as “*Free convection boiling*”. FCB starts at saturation temperature and exists up to the point where $\Delta T_e \approx 5^{\circ}\text{C}$. It can be also stated that FCB shows the weakest signatures of the boiling. Transfer of the heat is available by rising hot medium because of decreasing density of the fluid. There is no bubble occurrence. Therefore, this region is named under free convection phrase.

The second mode of the boiling is “*Nucleate Boiling*”. Rather than FRB, strong visual evidence of boiling can be observed in NB. NB is present between $5^{\circ}\text{C} < \Delta T_e < 30^{\circ}\text{C}$ and there is a sharp increase in the amount of maximum heat can be transferred.

Nucleate boiling regime, however, has been subdivided into two categories because; the dominant heat transfer mechanism differs with increasing temperature. In the Figure 2.7, from A to B is named as partial nucleate boiling. The reason for this designation is that even bubble formation or alternatively nucleation takes place in this region; the heat transfer can be supplied by rising bubbles to the top. Therefore, the dominant mechanism of heat transfer is caused by decreasing buoyancy because of bubble formations. Nevertheless, heat is transferred through bubble movement. Consequently, this is not free convection or forced convection so, it is named as partial nucleate boiling or isolated bubbles region. It roughly occurs at $5^{\circ}\text{C} < \Delta T_e < 10^{\circ}\text{C}$.

The other dominant mechanism, following after partial nucleate boiling, is forced convection due to slugs of jet and columns of vapor. After a certain temperature difference, $\Delta T_e \approx 10^{\circ}\text{C}$, nucleation is so fast that bubbles form a huge chain from the heated surface to the top. There is an enormous rate of heat transfer through this coalescence and this is pure convection. As a result, this condition is distinguished as fully developed nucleate boiling.

After completing NB region, the boiling curve reaches peak, depicted as “*Critical Heat Flux*”. CHF is the maximum amount of heat can be transferred by boiling process. CHF is a very crucial parameter for an engineering problem since; there is a drastic drop of convection coefficient beyond this point. CHF is highly unstable point and for a safe operation a system should operate below CHF. Nonetheless, design must be close enough to CHF for optimal conditions.

For CHF, Kutateladze [15] and Zuber [16] offer an expression in this form:

$$q''_{\max} = C_p h_{fg} \rho_v \left[\frac{\sigma g (\rho_l - \rho_v)}{\rho_v^2} \right]^{1/4} \quad (2.5)$$

Equation 2.5 is the most primitive form of CHF. It can be called as primitive because, lots of important parameters, such as geometrical, material properties, surface quality, subcooling

degree etc., are not considered. Kandlikar [17] has underlined that a CHF equation should consider all of the mentioned parameters above.

Instead of Equation 2.5, a recent CHF equation is [17]:

$$q''_{\max} = h_{fg} \rho_v^{1/2} \left(\frac{1 + \cos \beta}{16} \right) \left[\frac{2}{\pi} + \frac{\pi}{4} (1 + \cos \beta) \cos \theta \right] [\sigma g (\rho_l - \rho_v)]^{1/4} \quad (2.6)$$

In Equation 2.6 contact angle of wetting and surface orientation are considered. Nevertheless, subcooling degree is an important parameter when considering CHF for that reason it has to be added into a CHF equation. If q''_{\max} is modified by subcooling effect, following relation appears:

$$q''_{\max,sub} = q''_{\max} \left(1 + \frac{\Delta T_{sub}}{\Delta T_e} \right)_{sub} \quad (2.7)$$

The other two modes of two-phase heat transfer are “*Transition Boiling*” and “*Film Boiling*”, consecutively. “*Transition Boiling*” is also defined as unstable film boiling or partial film boiling. TB occurs between point “C” and “D” in the boiling curve. These points refer to 30°C and 120°C in Nukiyama’s experiment, respectively. Oscillated transition of film and nucleate boiling is the main reason for calling this region as unstable. A vapor film is established on the surface which brings about of abrupt drop of convection coefficient. The vapor film catalysts a huge thermal resistance when compared to liquid phase. Therefore, a sharp temperature gradient takes place which is the result of low degree of heat transfer.

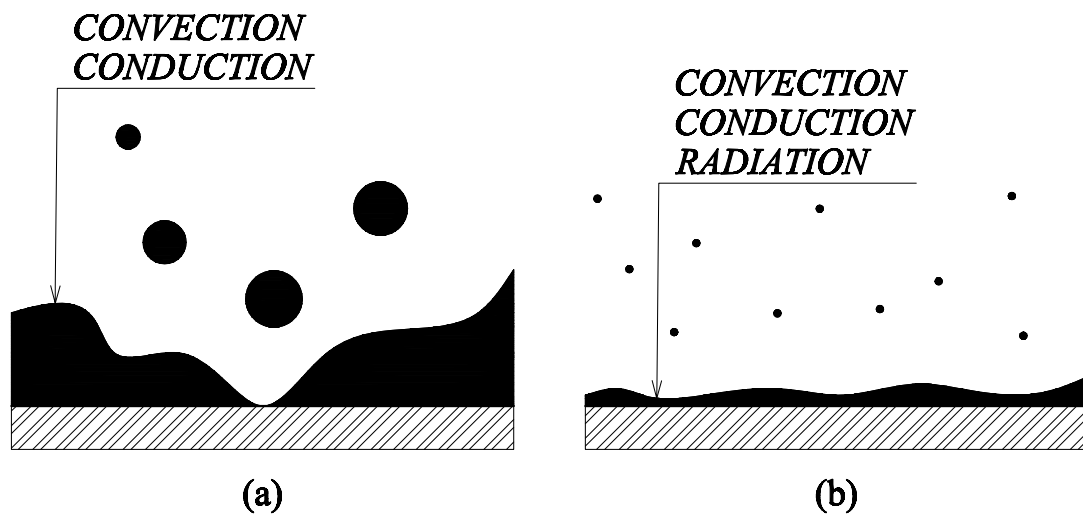


Figure 2.8: (a) Transition boiling (b) Film boiling

The point “D” on the boiling curve is named as *Leidenfrost point* where minimum amount of heat is transferred by two-phase heat transfer.

The final boiling region, after TB, is termed as “*Film Boiling*”. In FB region, ΔT_e is larger

than 120°C . FB regime is generally observed at metal quenching processes. For that reason, order of the surface temperatures are very high compared to FCB, NB and TB so, radiation is the dominant heat transfer mechanism in FB. In FB region, a thin film stays on the heated surface. Unlike TB, there is no a sharp temperature gradient since, the heat of surface is radiated through ambient. Therefore, CHF of FB region has an increasing trend as the ΔT_e increases. It will not be wrong statement that conduction and convection through the vapor film and rising bubbles are the main heat transfer mechanism of TB alas; radiation enhances higher degree of heat transfer due to high surface temperature in FB. This is the explanation of how TB gets steady.

2.4 Literature Review of Spray Cooling Applications

In heat transfer literature, spray cooling applications cover a wide area. Lots of experimental and numerical studies are present. These studies have various focuses ranging from quenching steel bars to dermatologic cryogenic cooling. The interesting point about spray cooling technique is that most of the papers published recently are concentrated on electronics cooling application. Therefore, lots of numerical and experimental references are available.

Issam Mudawar and his team mainly aim to find a general correlation for determining CHF of a spray cooling system at nucleate boiling region. Effects of parameters such as inclination and overlapping of sprays, subcooling degree of fluid, type of fluids, surface quality etc. are observed in experiments and compared with correlated ones.

The most updated version of experiment setup that is used in those studies has the following scheme:

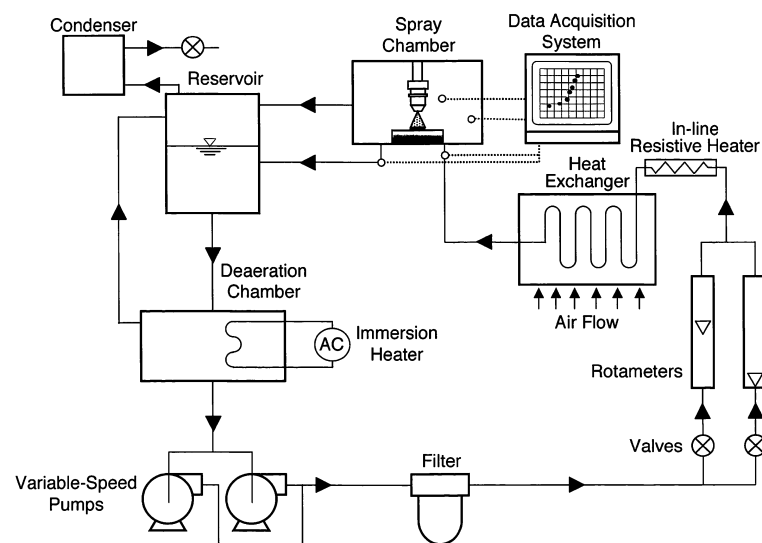


Figure 2.9: An example for spray cooling experimental setup [18]

In this spray cooling experimental setup a closed loop is preferred. Pressure line is fed by internal gear pumps. Spraying chamber is connected a cold sink, condenser side, to accomplish liquidation of gas in chamber. Additionally, temperature and pressure data are collected at the inlet and outlet ports of spraying chamber.

Although the most preferred experimental setup design is similar to form in Figure 2.9, open loop experimental setups are also built up. They are less complicated however; continuous fluid supply has to be present. Nevertheless, higher pressure rates compared to internal gear pump case can be reached by an external pressurized gas supply [19].

The next important parameter for a spray cooling experiment setup is designing heating block. Heating block must be carefully designed and produced so that heat loss through ambient is minimum. For that specific reason high temperature resistant insulation materials are widely used.

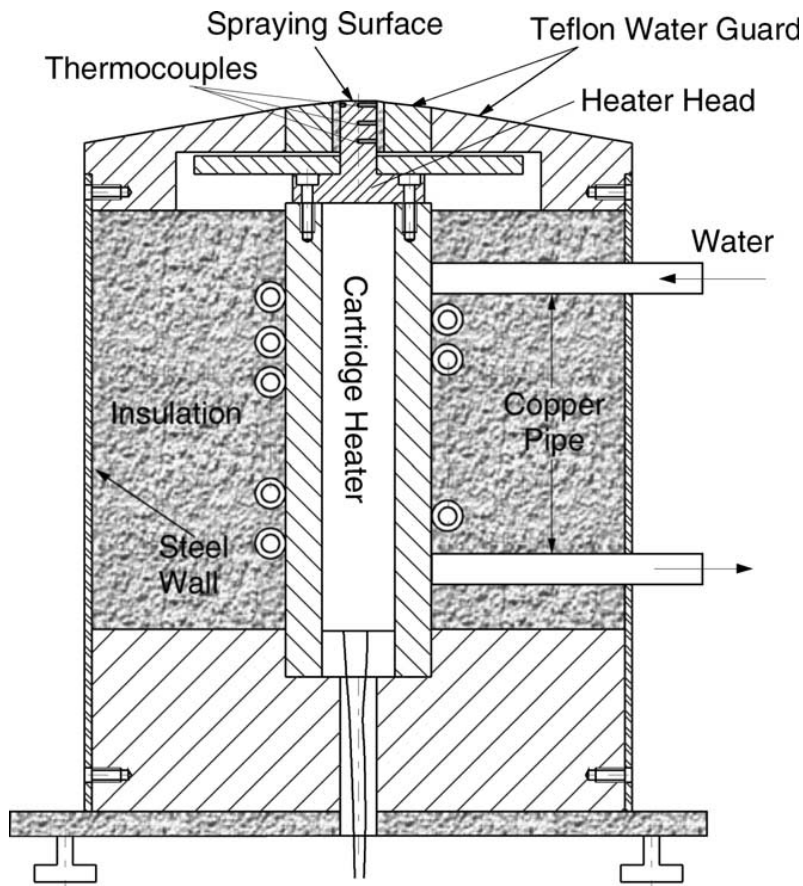


Figure 2.10: A well insulated sprayed surface [20]

For observation of geometric parameters, different spraying angle should be offered at a good spray cooling experiment setup. Spraying angle directly determines how large a cooling package will be built. There has been lots of research to find out how heat transfer coefficient change with different orientations. Moreover, height of spray head should be adjustable

since; spraying cone forwarded to heated area must enclose fully the heated area for acquiring trustful temperature data. Different angle spraying can be either a moving mechanism or steady manifold.

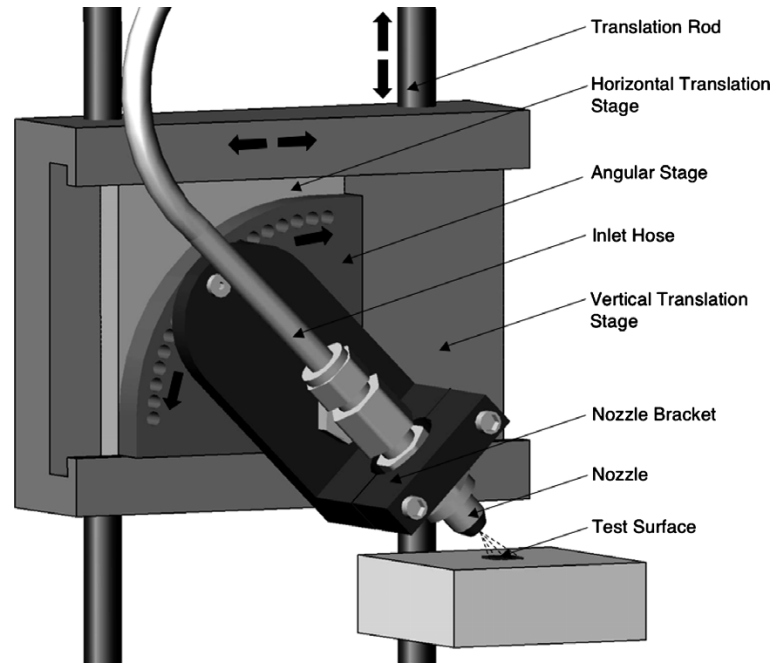


Figure 2.11: Adjustable angle mechanism for a spray cooling setup [21]

Spray cooling systems utilize many kind of fluid for heat transfer. Dielectric fluids, compatible with electronic assemblies, are mostly preferred ones for their special characteristics. Water is also used in so many experiments. Nonetheless, its boiling temperature and destructive effects on electronics do not let it to be used with electronics cooling. Water sprays are mostly used quenching bars going through extrusion [22].

On the electronics cooling side there are bunch of study brought about by scientists and engineers. Voltage converters and power amplifiers are very sensitive to high heat flux because when their junction temperatures exceed design temperature their efficiencies drop significantly. Moreover, high heat flux can destroy them. Spray cooling is a suitable cure for this type of assemblies.

Cotler et al. have studied on spray cooling of a LD-Mosfet RF power amplifier [23]. In this study, efficiency of power amplifier is increased from 26% to 34%. Besides, thermal resistance is decreased from $1.5^{\circ}C/W$ to $0.6^{\circ}C/W$. As a matter of fact, this kind of study can enhance a military device's range in battlefield so that one having spray cooling technology on military devices can dominate others. Mertens et al. have also cooled down an IGBT device by spray cooling [24].

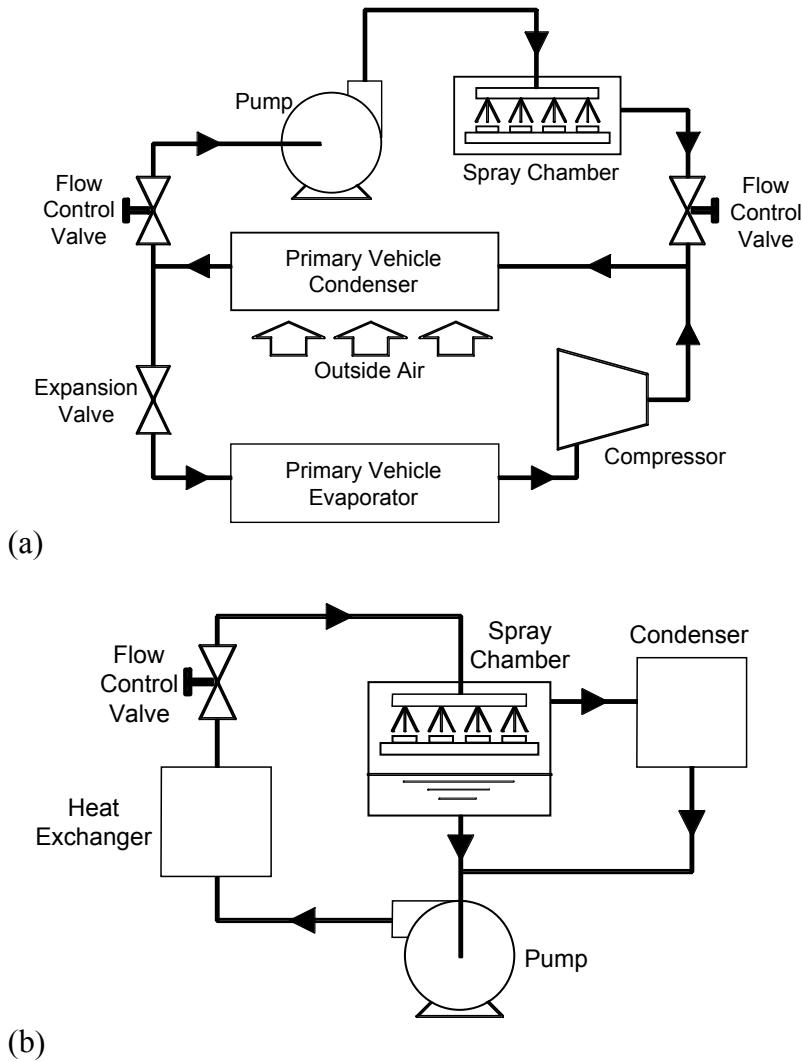


Figure 2.12: Cooling of hybrid vehicle power electronics by (a) modifying existing R134a air-conditioning refrigeration loop and (b) using a separate cooling loop with appropriate coolant [25].

Spray cooling technology can be most preferred cooling technique for the future. Hybrid cars or purely run electric cars are realized perfect replacements for cars using petroleum because; it is generally stated that fossil fuels are about to run out. In addition to this, they are also nature friendly. Nevertheless, they are also susceptible to high heat fluxes. Furthermore, the range of electric cars directly depends on how much electronics parts placed into them are efficient. All in all, it can be easily interpreted that range of an electric car can be increased by integration of spray cooling. Mudawar et al. have looked for the feasibility of application of spray cooling in a hybrid car [25].

Visualization of spraying is another field attracting many attentions. Spraying chamber and area are generally expected to be crowded by so many droplets. Fluid stream coming out from nozzle, or atomizer, is scattered into so many little droplets and spread out. For that reason,

it is almost impossible to observe spraying by naked eyes. Therefore, special instruments and techniques are widely used in literature for watching droplets. Horacek et al. have used high speed camera to visualize sprayed droplets by using total internal reflectance (TIR) technique.

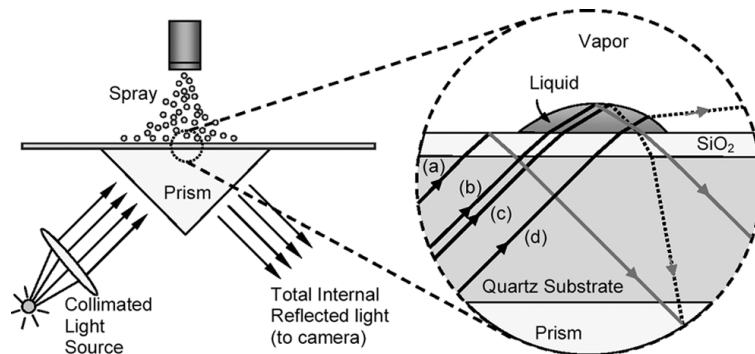


Figure 2.13: TIR (Total internal reflectance) technique [26].

Ortloff et al [27] have forwarded their attention to visualization of single droplet. They have carried out their studies both experimentally and numerically and then compare each other. Their main aim is matching the CFD analysis with experimental results. Both flow and heat transfer equations are solved. As a final word, they have stated that a single sprayed droplet have a different spreading character on a surface depending on wetness, hot-cold case and mass flow rate.

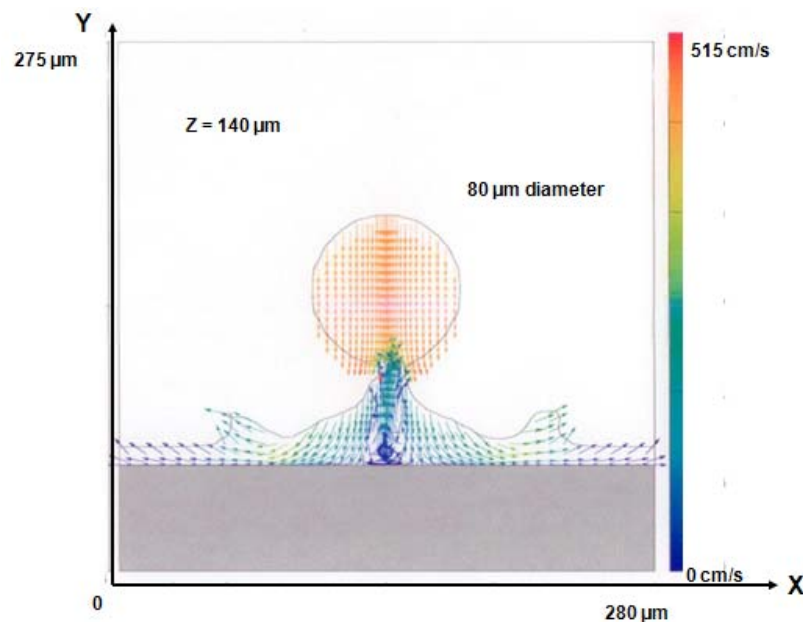


Figure 2.14: Velocity vectors of a single droplet through a CFD analysis [27].

Bernardin et al [28] have drawn a figure depicting a transient impact characteristic of a single water droplet. This transient history of a single water droplet is created for a fixed $We = 20$.

The figure contains images for both nucleate boiling and film boiling.

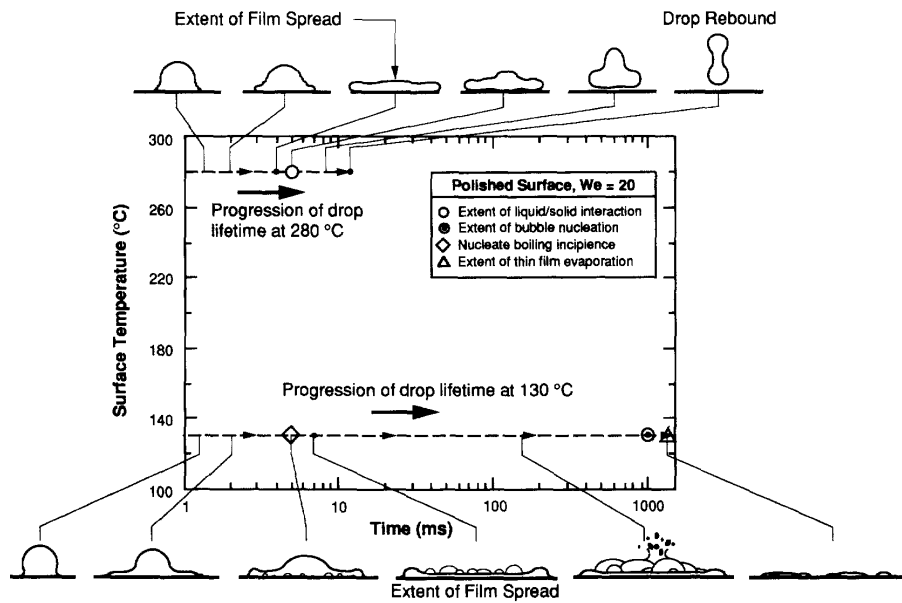


Figure 2.15: Impact history of a water droplet for fixed $We_l = 20$ [28].

Most of the researchers have focused on how spray cooling performance will be affected with varying parameters. Those parameters cover a huge list such as geometric, mechanical, material conditions etc. Nevertheless, after a careful investigation on literature, following conditions have taken more attentions than other: Spray angle, subcooling degree of fluid, surface conditions, nozzle inlet pressure or mass flow rate and nozzle arrangements (single, multiple, overlapping etc.)

Silk et al. [10] conducted experiments for four different spraying angles, 0° , 15° , 30° and 45° . In those experiments, surface patterns were also altered to determine their effects on CHF. At the end of tests, it was observed that CHF was almost same for 0° , 15° and 30° . It dramatically dropped when the normal is 45° , though. In this study, different surface geometries are manufactured to realize their effects to CHF. They have increased boiling efficiency from %29 to at most %46 by using straight finned surfaces.

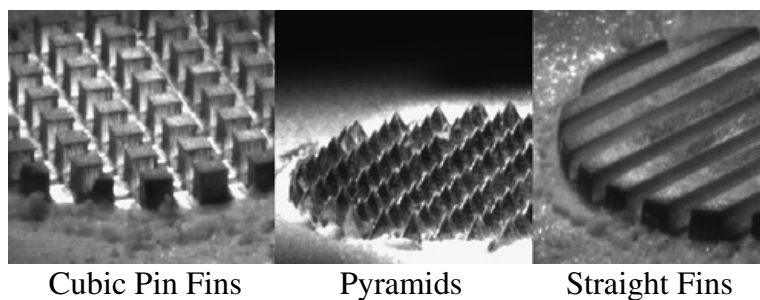


Figure 2.16: Different shapes of enhanced surfaces [10].

A similar work has brought about by Visaira and Mudawar, too. They have worked on angles from 0° , 10° , 25° , 45° and 55° , with PF-5052 fluid. Very close results, when compared with Silk et al., have been obtained.

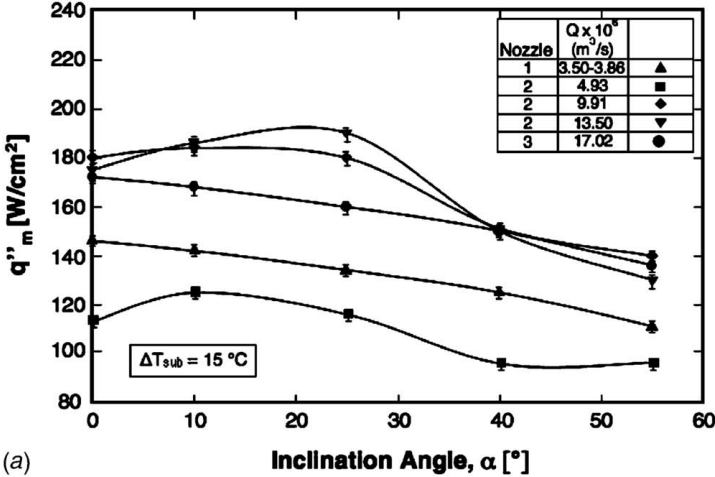


Figure 2.17: Angle and chf relation [29].

Subcooling degree of a fluid can be defined as the temperature difference between current state and boiling point. Subcooling degree of a spraying fluid plays crucial role at cooling performance. Fluid temperature is rising up to boiling point and heat transfer is dominated by constant specific heat, C_p . This mechanism is related with Ja number, too.

Visaira and Mudawar have selected dielectric fluid FC-77 for its high boiling point, $97^\circ C$, so that they can test subcooling for a wide range [30]. In this study, it was showed that CHF of FC-77 can be increased up to 100% by increasing subcooling from $22^\circ C$ to $77^\circ C$. At the same study, CHF was also folded by increasing mass flow and decreasing droplet size. They have also modified their empirical CHF equation with new subcooling effect. Rather than spray cooling, subcooling effects are studied for different boiling mechanism, such as immersion cooling. El-Genk and Parker have studied subcooling by using dielectric fluids FC-72 and HFE-7100 [31]. In this study, porous graphite has been used for immersion cooling. At the end, they have stated that increasing subcooling decreases total heat transfer coefficient, but increases boiling heat transfer and CHF value. For that reason when defining a heat transfer coefficient for a spray cooling application, it has to be carefully noted that whether heat transfer coefficient covers boiling regime or all regimes, sensible heating and phase change.

Most of the spray cooling applications utilize a single nozzle. Unluckily, it is almost impossible to have a single hot spot and a single nozzle for cooling down a real problem. Most of the electronic PCB or cold plates accommodate lots of problematic hot spots into itself. Pautsch and Shedd [32] have designed a nozzle manifold containing lots of orifices. In their design, they have claimed that they have increased CHF when comparing to commercial nozzle ones.

Fabbri and Dhir [33] have also tested experimentally single phase spray cooling by using multiple microjets. They have used FC-40 dielectric fluid. An empirical correlation is derived for three dimensional spraying applications.

Until this point, spray cooling applications with conventional actuation mechanism are discussed. Conventional actuation mechanisms mean driving nozzles with continuous supply of fluid. Nevertheless, recent applications and studies point out that CHF and boiling efficiency can be increased by pulsed sprays [34]. In those studies, it is observed that vapor is removed more rapidly when comparing to continuous operation. As a result, CHF is increased by driving nozzles between 10-30 Hz. Another interesting work about intermittent spray cooling is driving multiple nozzles intermittently by electrospray [35]. In this study, droplets are charged electrically so that rebounding from the surface is minimum. When charged droplets hit the heated surface, it is easier to break surface tension forces by electrocharging. Therefore, cooling efficiency is increased. Furthermore, intermittent regime is applied. As a result, 96 W/cm^2 is cooled down with 97% boiling efficiency. Commercial products such as inkjet printers are also used in spray cooling applications [36]. With this products, spray cooling is achieved at very low volumetric fluxes.

Gravitational effects on spray cooling are also investigated by researchers [37]. In this study, boiling curves for both water and FC-72 are obtained at relatively low volumetric fluxes, about $2 \text{ ml/cm}^2\text{min}$. Gravitation is also altered from 0.1 g to 1.8 g . However, it is observed that boiling curve and CHF values are not affected. Besides, Kim [38] states that spray cooling performance is barely shifted under different g conditions for the reason that fluid particles are generally subjected to large momentums.

CHAPTER 3

EXPERIMENTAL SETUP AND PROCEDURE

3.1 Designing of a Spray Cooling Experimental Setup

Designing an experimental setup demands great care without hesitation. It has to be well planned and built even it serves for a very simple aim. The following properties can be addressed for a good engineering experimental setup:

1. **Simplicity:** An experiment setup has to be simple as much as possible. The simplicity of an experimental setup does not mean omitting parts that are complex. Simplicity in an experiment covers easy mounting and dismounting, using parts require low level skills, cheap and basic maintenance costs and using parts with enough abilities.
2. **Measurability:** An ideal experimental setup makes it possible to measure variables at desired points. Necessary ports for measuring instruments must be supplied. Additionally, measurements devices and results do not interfere with each other at a good experimental setup. For the sake of first rule of a good experimental setup, measurements have to be only carried out at necessary points. Usage of calibrated and certificated measurement instruments are always a must for accredited results. Calibration dates have to be periodically checked.
3. **Repeatability:** An ideal experiment setup has to occupy minimum uncertainty so that results are independent of disturbances. In other words, every variable in experiments are under control. As a result, similar results are obtained providing that same inputs with previous experiments are supplied. First rule of a designing an experimental setup indirectly assist for this goal whereas, second rule directly determines availability of repeatability. All in all, repeatability of a system is indication of how much it is controlled.

In this study a spray cooling setup is designed. Main parts of the system are:

- Spraying chamber

- Pump
- Reservoir
- Mass flow meter
- Pressure transducer and pressure dial gage
- Thermocouples
- Data acquisition system
- Power supplies

The parts are assembled in the following form:

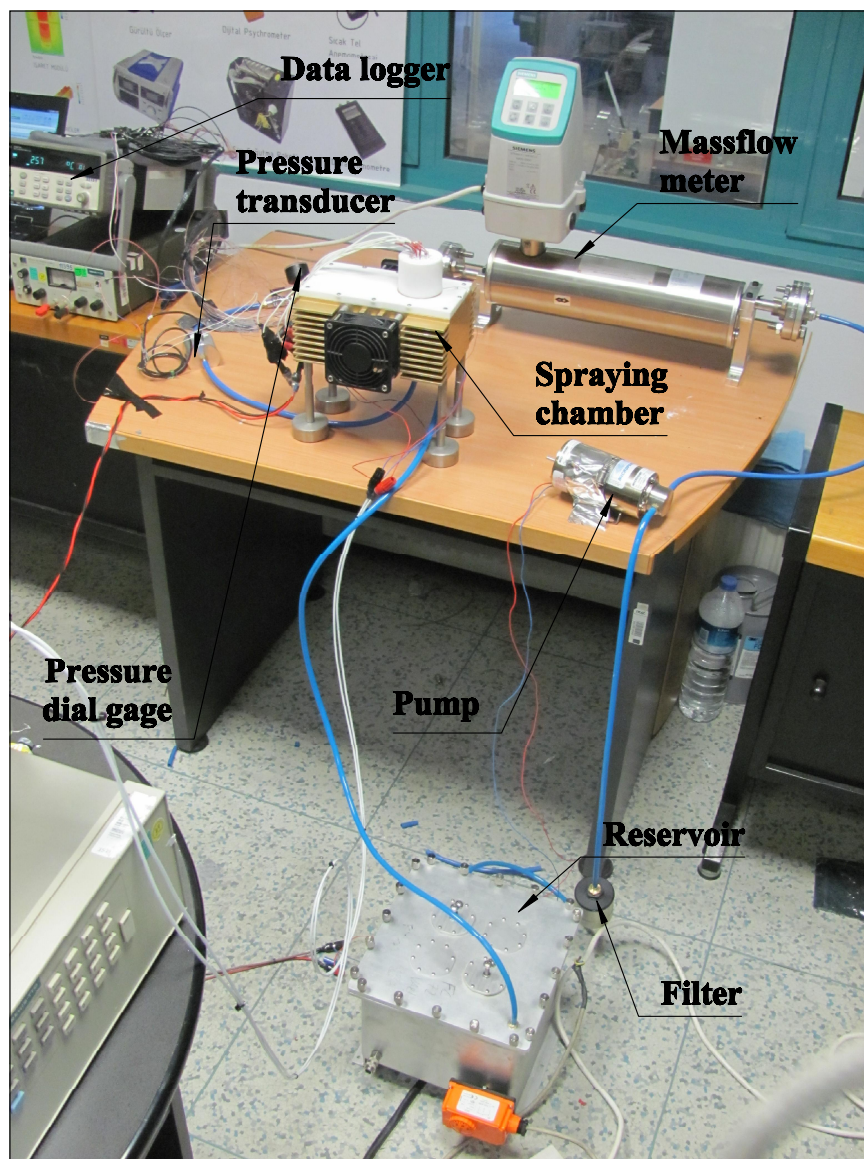


Figure 3.1: Overview of experimental setup

It is planned to create an experimental setup as simple as possible. Parts used in the setup are not complex and expensive, except for measuring devices. They can be easily modified in a basic machine shop without requiring high level experience. Pipelines in the system can be easily mounted and demounted. Measurement devices, power supplies and transducers are all calibrated at special calibration offices. Data is collected via digital data logger and all of them transferred to computer memory.

For a clear understanding of the system:

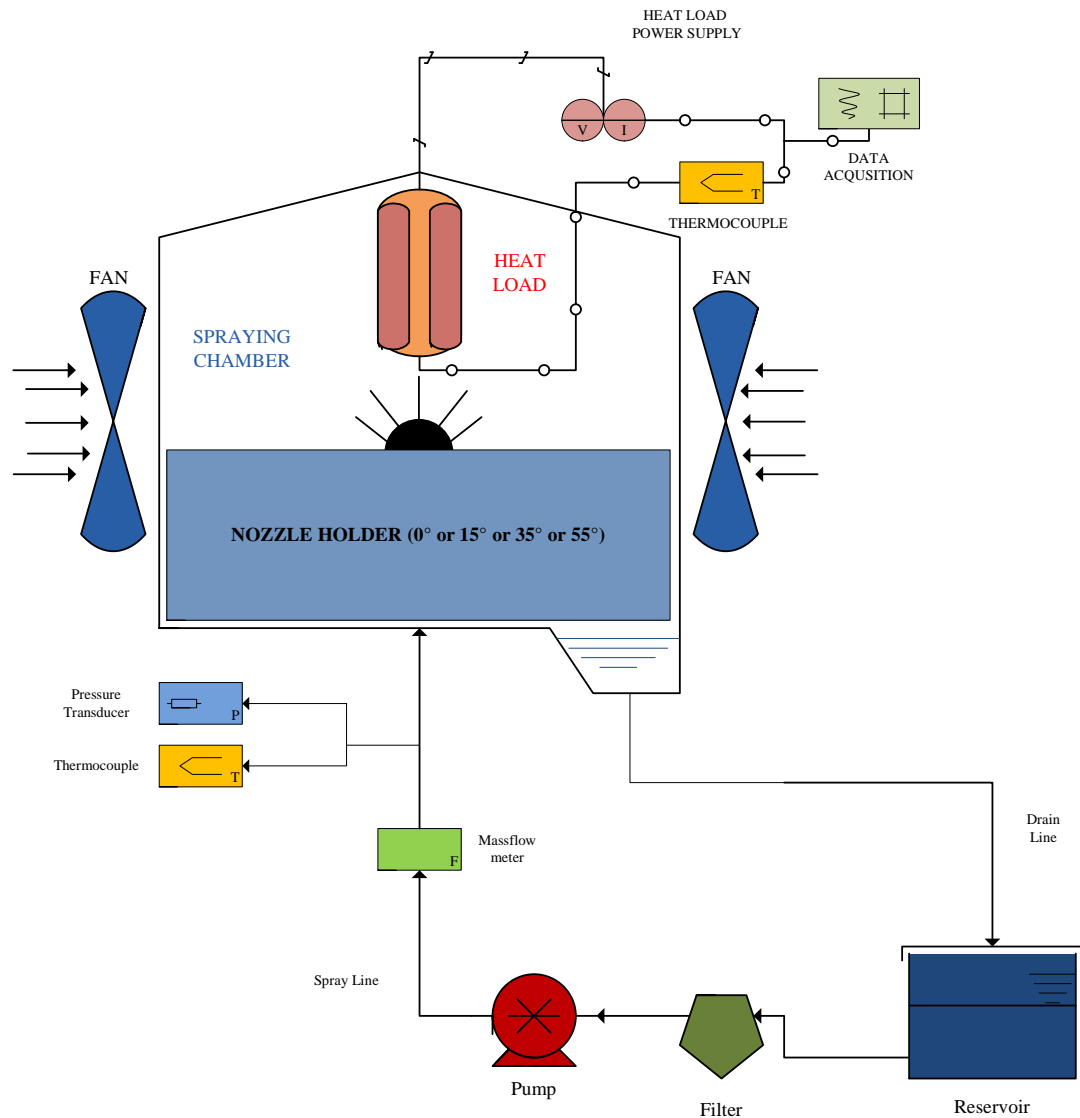


Figure 3.2: Spray cooling loop

The overall view of the system is in the Figure 3.2. From that point, it is more convenient to investigate experimental setup part separately.

The most complex part of the system is “Spraying chamber”. Spraying chamber has to be produced very precisely since the main data is collected from this volume.

Spraying chamber is produced from aluminum alloy 6061-T6 in a 3 axis CNC milling machine. The reason behind choosing aluminum alloy 6061-T6 is requiring high thermal conductivity for condensation of sprayed liquid.

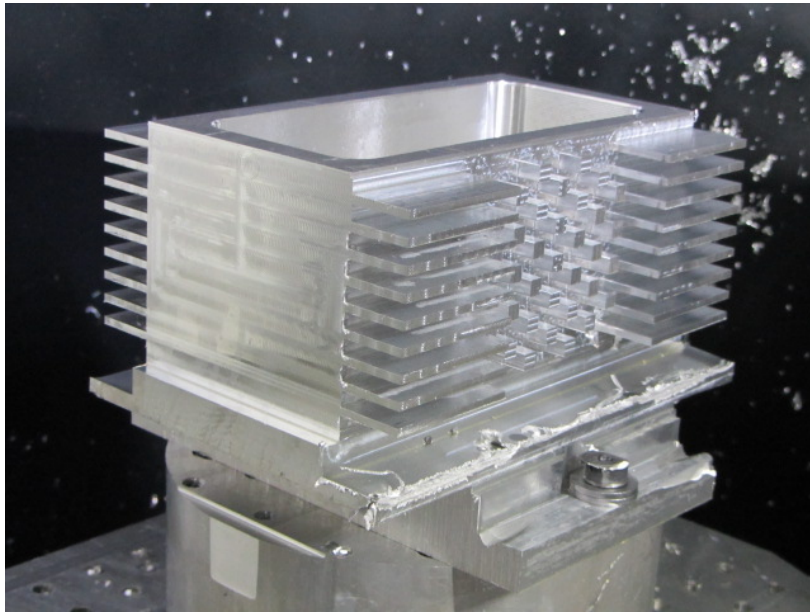


Figure 3.3: Manufacturing of spraying chamber

Spraying chamber carries a crucial role in the system. It has to provide sealing to system. The experimental setup is designed as closed loop. Therefore, leakage and outgassing precautions are strictly offered. Spraying chamber is designed so carefully to answer those needs. For that reason every part mounted on the spraying chamber has a sealing interface.

Another issue with the experimental setup is condensation of the sprayed liquid. The mist has to be condensed and be returned to reservoir. Two 13000 RPM axial fans are assembled on spraying chamber's extended surfaces. The fans constantly supply room air to surface of spraying chamber.

Spraying chamber contains spray holders at different angles. There are four different spray holders manufactured. These are 0° , 15° , 35° and 45° spray holders. Holders accommodate an inlet port through the nozzles. Pressure and temperature is recorded just before spray holders. Only one spraying holder can be placed in spraying chamber at the experiment time. For that reason, different spray holders are mounted and dismantled for desired angle of spraying.

Spray cooling chamber is closed with PTFE material whose commercial name is "Teflon". Teflon is a very important for this experimental setup. Firstly, it can withstand up to temperature $200^\circ C$, which means sustaining same formation. Additionally, it has superior insulation material. By using Teflon at interfaces, heat loss to ambient is minimized. As a result, heat in the system is transferred by only spraying.

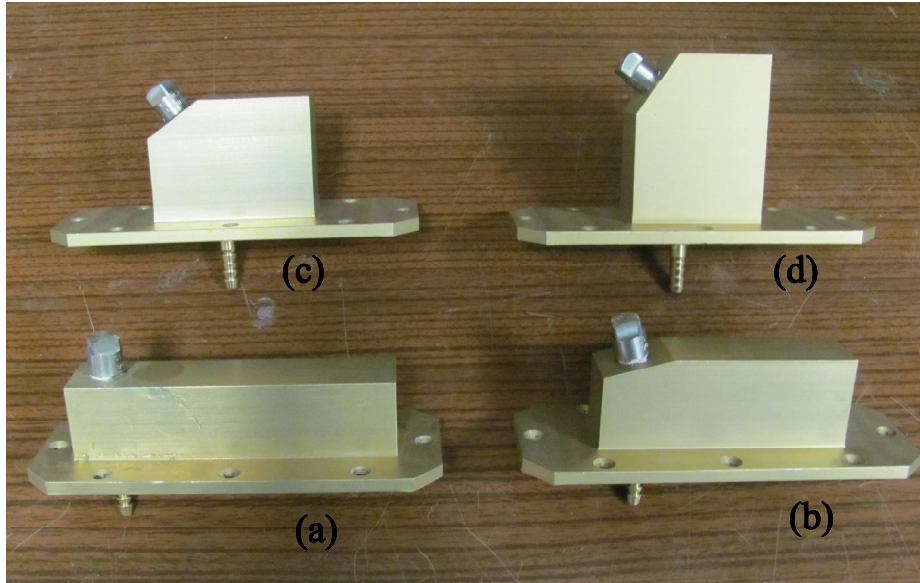


Figure 3.4: (a) 0° nozzle holder (b) 15° nozzle holder (c) 35° nozzle holder (d) 55° nozzle holder

Designing nozzle holders has required great attention. Sprayed liquid cone must enclose fully the surface to be cooled. If different spraying angles are present, the height and orientation of nozzle holders are different from each other.

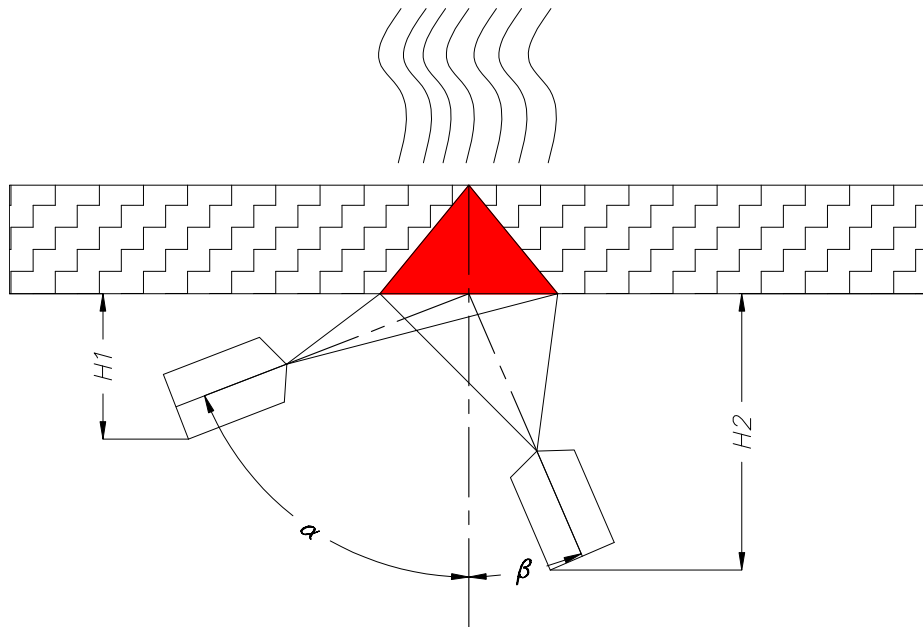


Figure 3.5: Designing spray holders

It is clearly explained in the Figure 3.5 how nozzle holders are designed for heated surface.

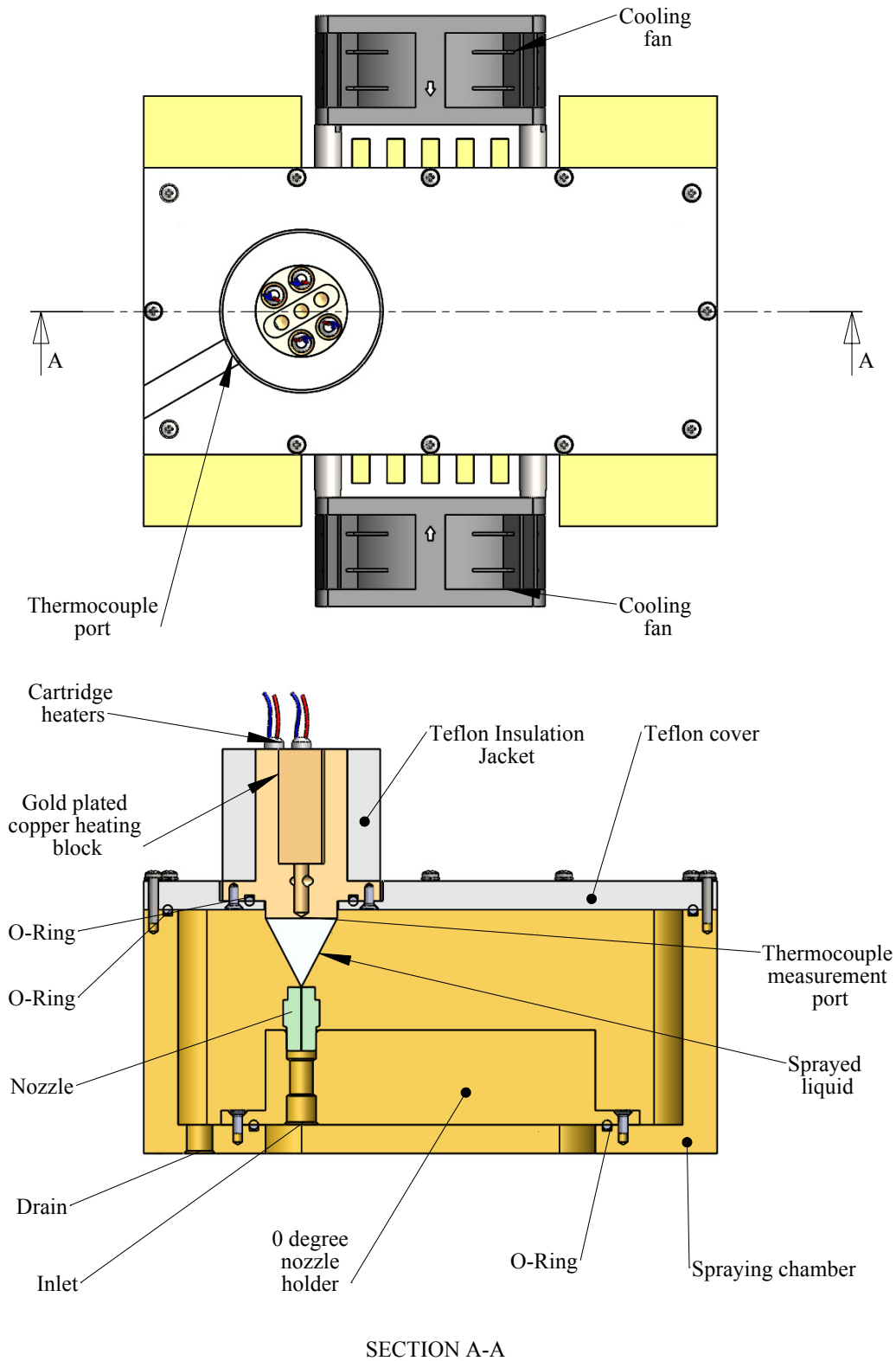


Figure 3.6: Detailed view of spraying chamber

Detailed view of spraying chamber is in the Figure 3.6.

Another important assembly in spraying chamber is heating block. Actually, heating block consist of 4 cartridge heater, which can supply 200 W heat load individually, gold plated copper block and insulation jacket.

Heating block is produced from copper to obtain low thermal resistance between surface and thermocouple port. Thermocouple port is 0.5 mm above surface. Nevertheless, in spray cooling experiments temperature is measured for detection of spraying CHF. If temperature rises so sharply, it means convection coefficient drops dramatically. In other words, boiling crisis is present in the system. In the heating block thermocouples are attached to ports by using special thermal greases. Heating block has a 25 mm diametered circle surface, stands for 4.9 cm^2 surface, which is covered by spraying cone fully. Additionally, a Teflon thermal insulation jacket is fitted on heating block to minimize heat loss through ambient. Heating block carries O-ring channel for sealing. It must be noted that special gaskets have to be selected whose outgassing ratio is low since boiling always takes place around this region.

Nozzle or atomizer in this experiment is produced by Spraying Systems Company. Its type number is 1/8 HSS Full Cone Spray Nozzle. It supplies 55° angle. The nominal orifice diameter is 0.762 mm. It is produced from stainless steel therefore, corrosion is not an expected problem. Only possible problem is blockage of orifice. This problem can be handled by using a filter in the system.

Pump is responsible for supplying pressure to system. The pump is used in this experimental setup can supply 5 Bar pressure difference and it is an internal gear pump. Nevertheless, 3 Bar pressure difference is the maximum in this experimental setup due to reliability concerns of pump. At the pump inlet a filter whose meshes are knitted with 50 μm intervals is placed to protect pump's gear.

Reservoir of the system can accumulate liquid up to 7 liters. The pressure on the reservoir is kept constant, equal to atmospheric pressure, by using spring loads. The condensed liquid is collected to reservoir by help of elevation difference between spraying chamber and reservoir. Reservoir of the system is made from aluminum alloy AA-5083 and plated by white chromium.

The reservoir capacity is selected big when compared to spraying capacity. The maximum flow can be reached in the system does not exceed 0.6 LPM. This means that liquid in the reservoir needs at least 10 minutes for being fully circulated. This difference between spraying capacity and reservoir volume causes that reservoir behaves as good source. In other words, temperature of the reservoir can be kept constant even large amount of heat is dissipated.

The other important parts of the system are measuring devices. In this experimental setup, mass flow, pressure, density and temperature can be recorded by different devices and transducers.

Mass flow meter can measure fluid temperature, mass flow in terms of kg/h and density of fluid by using Coriolis effect. Pressure is measured by both electrical resistive type pressure

sensor and fluid resistive pressure dial gage. The electrical resistive type pressure sensor can also measure temperature.

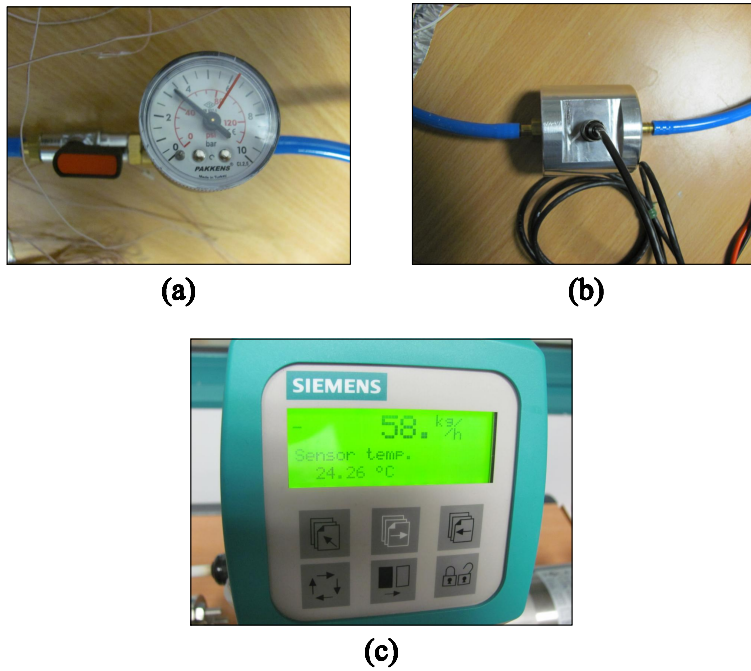


Figure 3.7: (a) Pressure dial gage (b) Electrically resistive pressure and temperature transducer (c) Mass flow meter

The other supplying instruments in the experiment setup are power suppliers. Power suppliers are transfer power to heat load, transducers and measurement devices, pumps and fans.

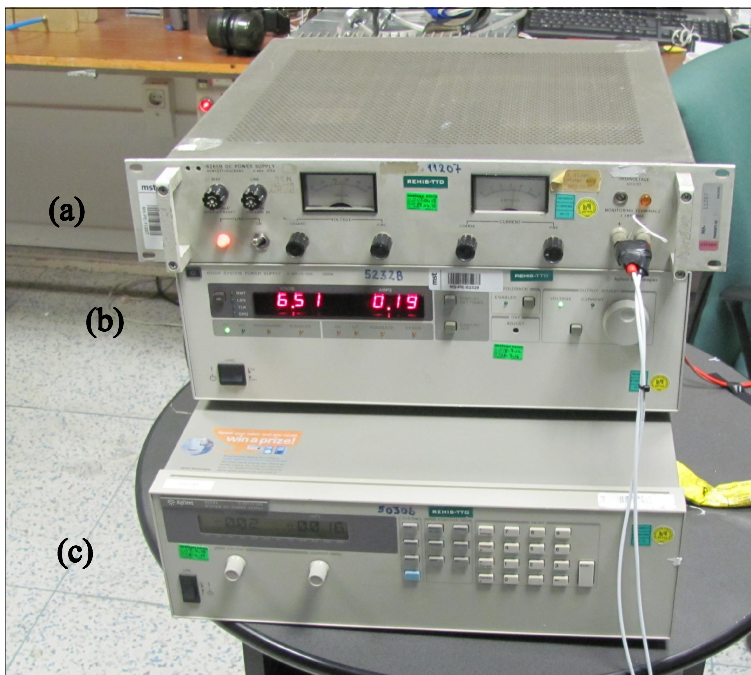


Figure 3.8: (a) Fan supply (b) Pump supply (c) Heat load supply

Sensors are fed by a 35 W power supply. A 100 W supply is used for fans. Pump is wired to a 1000 W capacity power supply. As it is expected, heat load supply can power out 3000 W. All of them operates in DC current.

3.2 Experimental Procedure

Starting with flowchart of the experiment is meaningful for better understanding.

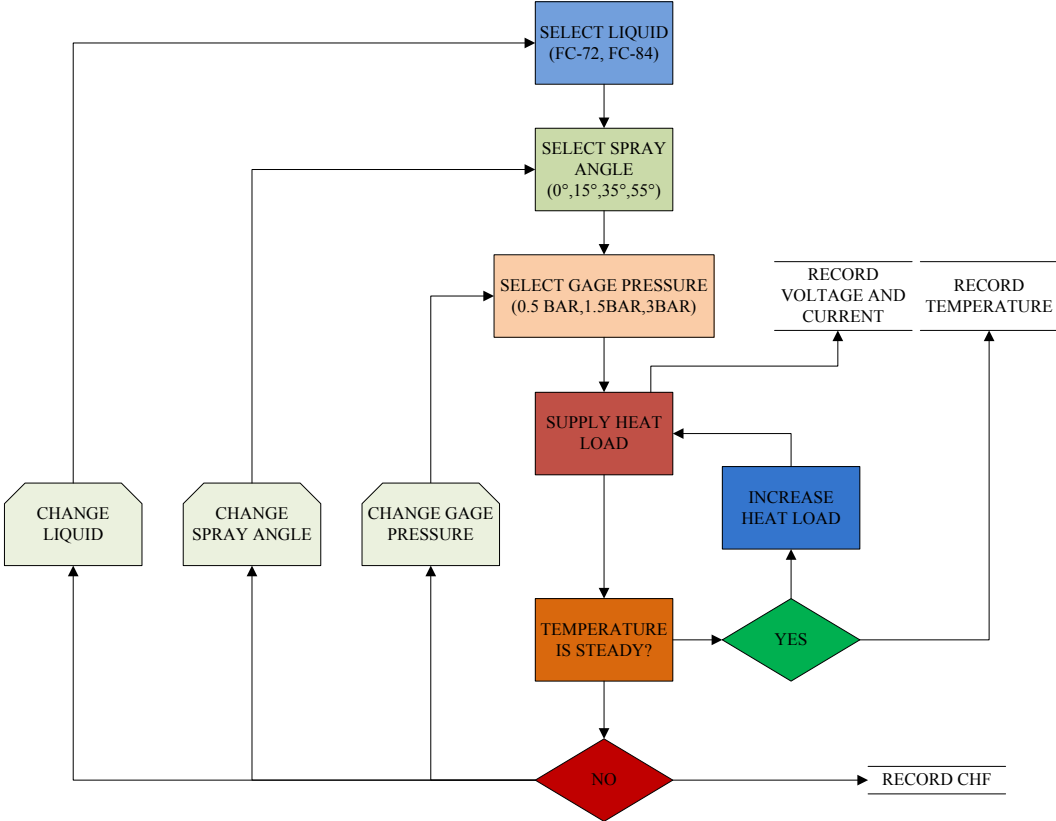


Figure 3.9: Flowchart of the experiment

It is visualized in Figure 3.9 how experimental procedure have taken place. As a first step of the experiment, type of the liquid is selected. In this experiment, two different dielectric fluids are available. The dielectric fluids are called with their commercial names.

At the second step spray angle is altered by different nozzle holders. There are four different angled nozzle holders. Then the third step is supplying pressure to the system. In this experiment three different gage pressure points are offered. Nozzle in the system is subjected to 0.5 BAR, 1.5 BAR and 3 BAR pressure difference.

After completing these steps, power supplies are started to run. Heat input is channeled to system via cartridge heaters. At this step, voltage and current that are supplied are recorded for determining total heat supplied. Then, temperature is observed. If temperature follows a

steady trend, it will be recorded. However, if the temperature increases abruptly, this means that boiling crisis has been started. The heat flux at this step stands for spraying CHF. There is not a well defined temperature at this point, because temperature is not steady. However, the temperature where temperature curve starts to rise sharply can be accepted as spraying CHF temperature.

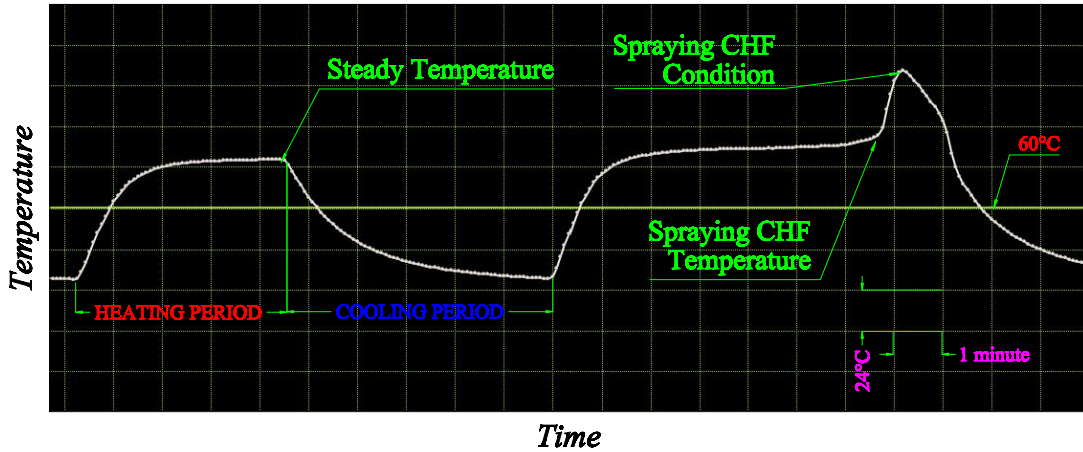


Figure 3.10: Transient raw data from data logger

In Figure 3.10 spraying CHF and steady state conditions are explained. Heating period of the system takes approximately 4-5 minutes, whereas cooling period is 1-2 minute longer than it.

The other important issue in the experimental procedure keeping reservoir temperature as possible as near the room temperature. The experiment place has an air conditioner which is set to 25°C. Air conditioner is started to run 2-3 hours before starting experiment.

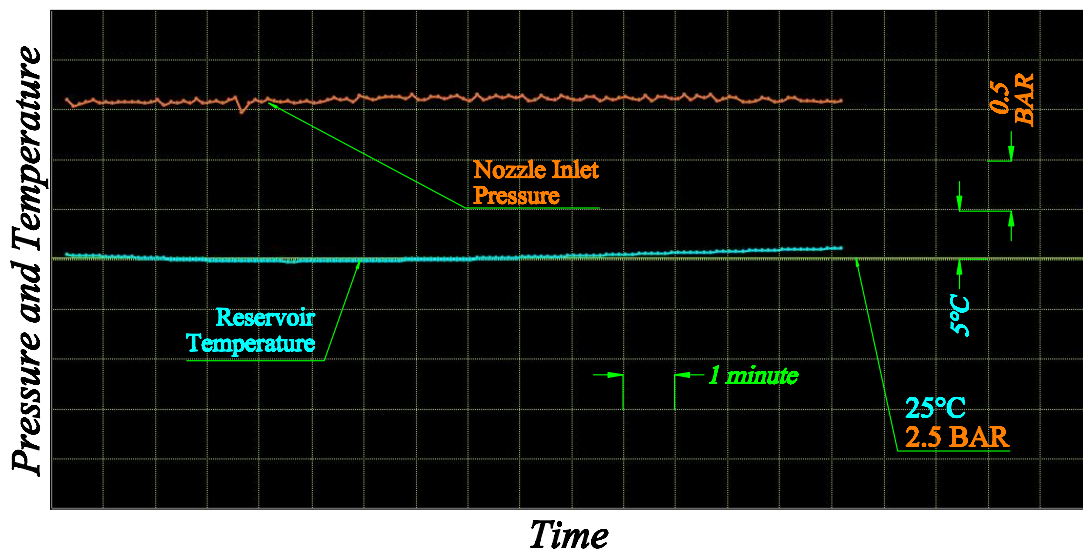


Figure 3.11: Transient reservoir temperature and nozzle inlet pressure

As it is interpreted from Figure 3.11, reservoir temperature is kept at 25°C region successfully.

At the uppermost pressure supply, pressure is oscillated as it is shown in the Figure 3.11. As a result, inlet temperature for all of the experiments is 25°C, and there is no significant pressure deviation rather than desired pressure value supplied. This may be the sign that experiment setup does not have cavitation for all the pressure values specified because, supplied pressure is almost constant.

From that point boiling curves for different fluids, different mass flows and different angles will be obtained.

The fluid properties at room temperature is tabulated in Table 3.1.

Table 3.1: Fluid Properties at 25°C and 1 ATM

FLUID PROPERTIES		FC -72	FC-84
T_{sat}	[°C]	56	80
ρ_f	[kg/m ³]	1697	1735
ρ_g	[kg/m ³]	12.4	4.4
σ_f	[N/m]	1.00E-02	1.20E-02
h_{fg}	[J/kg]	8.80E+04	9.10E+04
C_{pf}	[J/kgK]	1100	1095.6
μ_f	[Ns/m ²]	6.40E-04	5.79E-04

Air properties are also required for detecting breakup type. Air properties are given in Table 3.2.

Table 3.2: Air Properties at 25°C and 1 ATM

AIR PROPERTIES		
T	[°C]	25
P	[BAR]	1.01
ρ	[kg/m ³]	1.18
μ	[Ns/m ²]	18.48E-06

Other properties of the system are also important. At this point, they are tabulated, too.

Table 3.3: Other Properties of the System

Cone angle of nozzle	[°]	55
Orifice diameter	[m]	7.62e-04
Length of heated surface	[m]	2.5e-02
Inlet temperature	[°C]	25
Heated surface area	[cm ²]	4.91
ΔT_{sub} of FC-72	[°C]	31
ΔT_{sub} of FC-84	[°C]	55

After having listed all data above and having collected data from the experiment setup, they

have to be placed in meaningful graphs. For that specific reason, certain dimensionless numbers have to be specified. Those numbers will be specified are suitable for spraying applications.

As a first step d_{32} should be specified for spray cooling experiments. d_{32} is known as ‘‘Sauter Mean Diameter’’. Sauter Mean Diameter is generally used in fuel burning subjects. It is the ratio of volume to surface. SMD of a spray cooling application is derived by Estes and Mudawar [39].

$$\frac{d_{32}}{d_0} = 3.67 \left[We_{d_0}^{1/2} Re_{d_0} \right]^{-0.259} \quad (3.1)$$

Where;

$$We_{d_0} = \frac{\rho_a(2\Delta P/\rho_f)d_0}{\sigma_f} \quad (3.2)$$

$$We_l = \frac{\rho_l U^2 d_0}{\sigma} \quad (3.3)$$

and

$$Re_{d_0} = \frac{\rho_f(2\Delta P/\rho_f)^{1/2}d_0}{\mu_f} \quad (3.4)$$

Additionally:

$$We_a = We_{d_0} \quad (3.5)$$

And by using Equation 3.2 and Equation 3.4:

$$Oh = We_{d_0}^{0.5} Re_{d_0}^{-1} \quad (3.6)$$

Consequently, breakup regime can be found by using these equations.

Heat transfer coefficient can be found by following equations:

$$h = \frac{q''}{(T - T_{in})} = \frac{q''}{(\Delta T_e + \Delta T_{sub})} = \frac{q''}{((T - T_{sat}) + (T_{sat} - T_{in}))} \quad (3.7)$$

$$\Delta T_{sub} = T_{sat} - T_{in} \quad (3.8)$$

$$\Delta T_e = T - T_{sat} \quad (3.9)$$

CHAPTER 4

EXPERIMENT RESULTS

4.1 FC-72 Results

As a first step, important dimensionless numbers' values for FC-72 experiments are given in Table 4.1. Bold pressure values stand for the operation points in the experiments.

Table 4.1: Dimensionless Numbers for FC-72 Experiments

ΔP [Bar]	Q [m^3/s]	Re_{d_0}	We_{d_0}	We_l	Oh
0.4	3.43E-06	13873	4	7329	1.48E-04
0.5	3.77E-06	15510	5	8822	1.48E-04
0.7	4.58E-06	18352	7	13062	1.48E-04
1.5	6.87E-06	26864	16	29318	1.48E-04
2	7.85E-06	31020	21	38316	1.48E-04
3	9.17E-06	37992	32	52247	1.48E-04

The breakup regime and surface contact regime conditions are expected as given in Table 2.1 and in Figure 2.3, respectively.

Table 4.2: Breakup and Contact Regimes for FC-72 Experiments

ΔP [Bar]	Q [m^3/s]	Breakup Regime	Contact Regime
0.4	3.43E-06	First wind induced	Prompt splash
0.5	3.77E-06	First wind induced	Prompt splash
0.7	4.58E-06	First wind induced	Prompt splash
1.5	6.87E-06	Second wind induced	Prompt splash
2	7.85E-06	Second wind induced	Prompt splash
3	9.17E-06	Second wind induced	Prompt splash

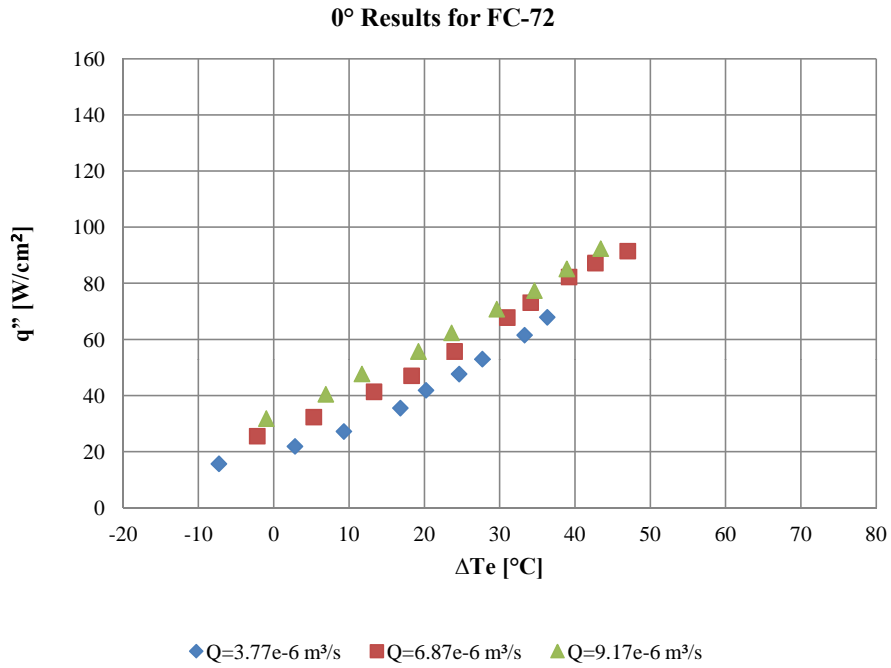


Figure 4.1: 0° boiling curve at different Q for FC-72

In Figure 4.1 it is observed, more heat can be transferred with increasing flow rate. Nevertheless, if breakup regime is shifted to next level, “Second wind induced” for example, heat transfer coefficient is increased more significantly. This is because of lower droplet size compared to previous breakup regime.

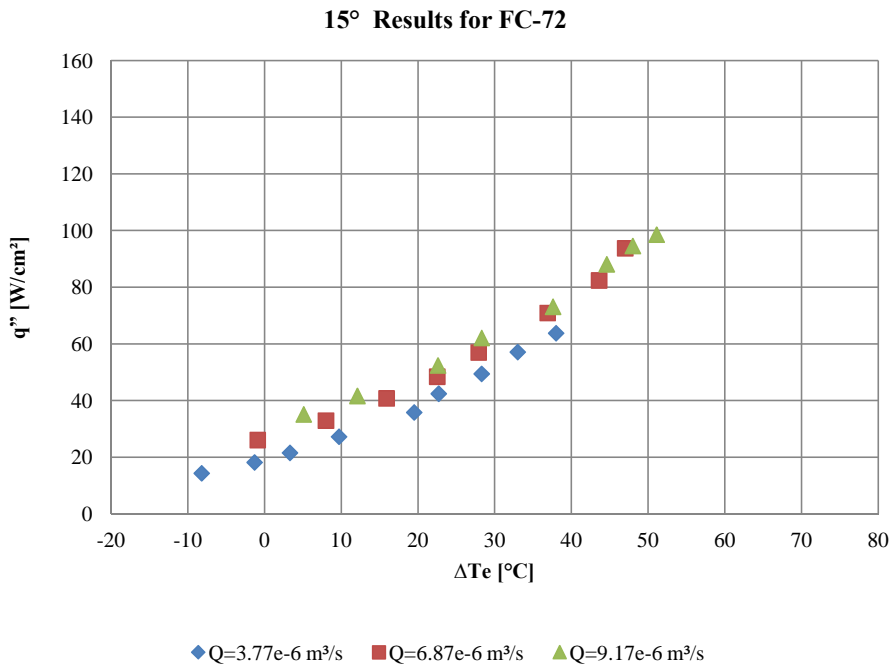


Figure 4.2: 15° boiling curve at different Q for FC-72

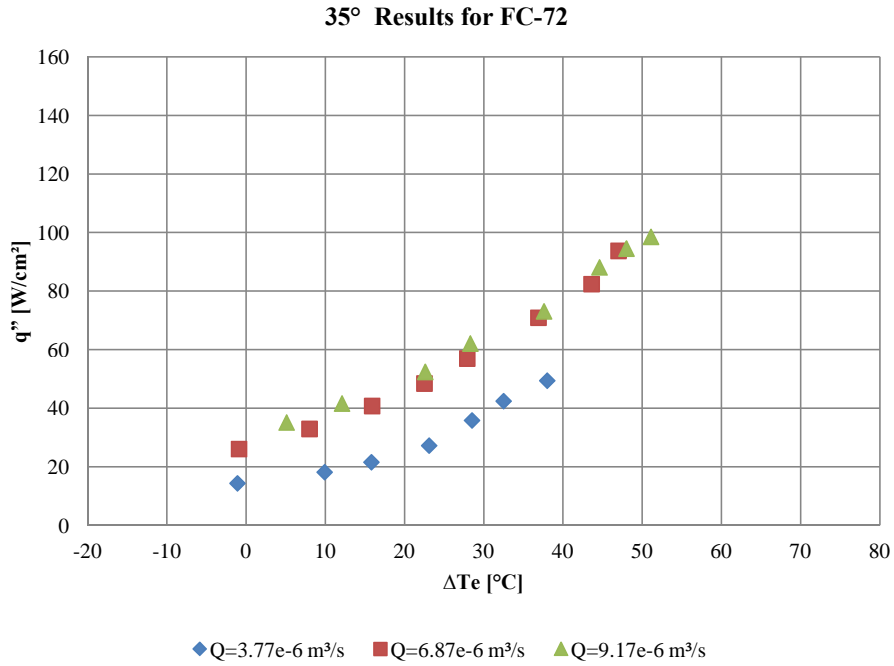


Figure 4.3: 35° boiling curve at different Q for FC-72

Figure 4.1 and Figure 4.2 have almost same characteristics for three different flow rates. In Figure 4.3, heat transfer characteristics are again similar with previous measurements. However, heat transfer coefficient at the smallest flow rate in Figure 4.3 is much more separated with other measurements at 35° when compared to previous measurements.

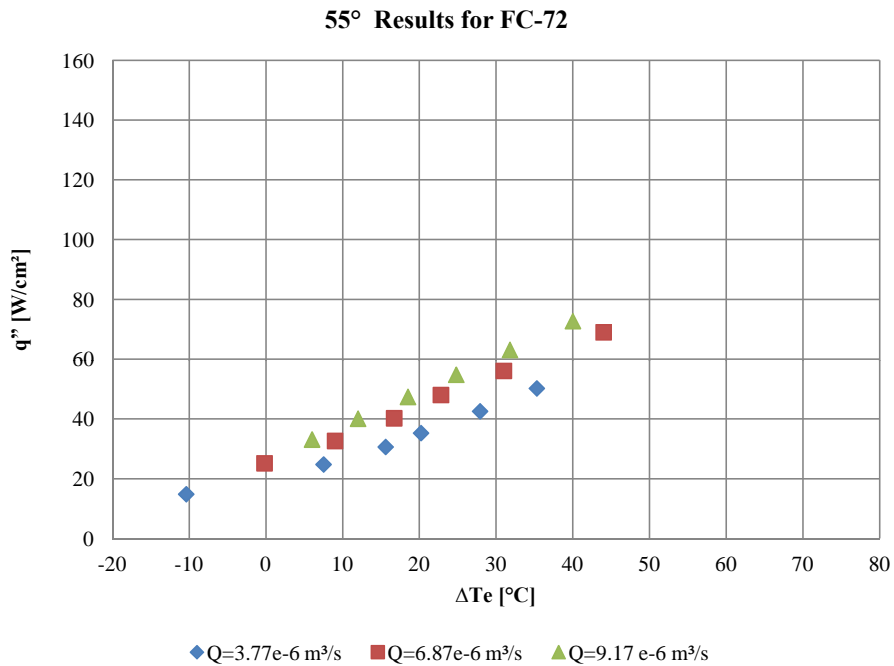


Figure 4.4: 55° boiling curve at different Q for FC-72

In Figure 4.4, heat transfer coefficient is much more lower than 0°, 15° and 35° results. Moreover, even flow rate is folded, heat transfer is not increased as in the former cases.

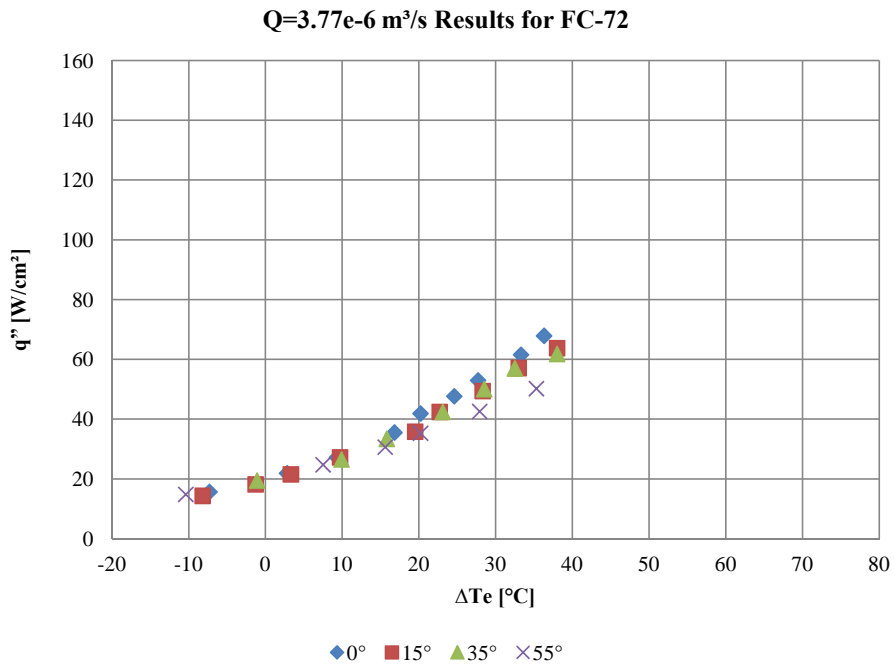


Figure 4.5: Boiling curves at different angles at $Q = 3.77 \times 10^{-6} \text{m}^3/\text{s}$ for FC-72

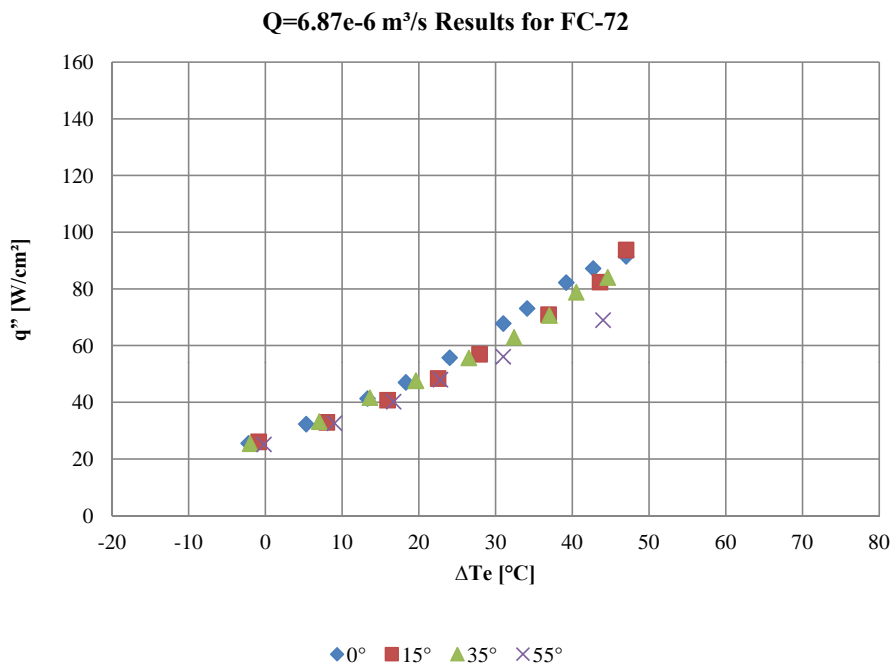


Figure 4.6: Boiling curves at different angles at $Q = 6.87 \times 10^{-6} \text{m}^3/\text{s}$ for FC-72

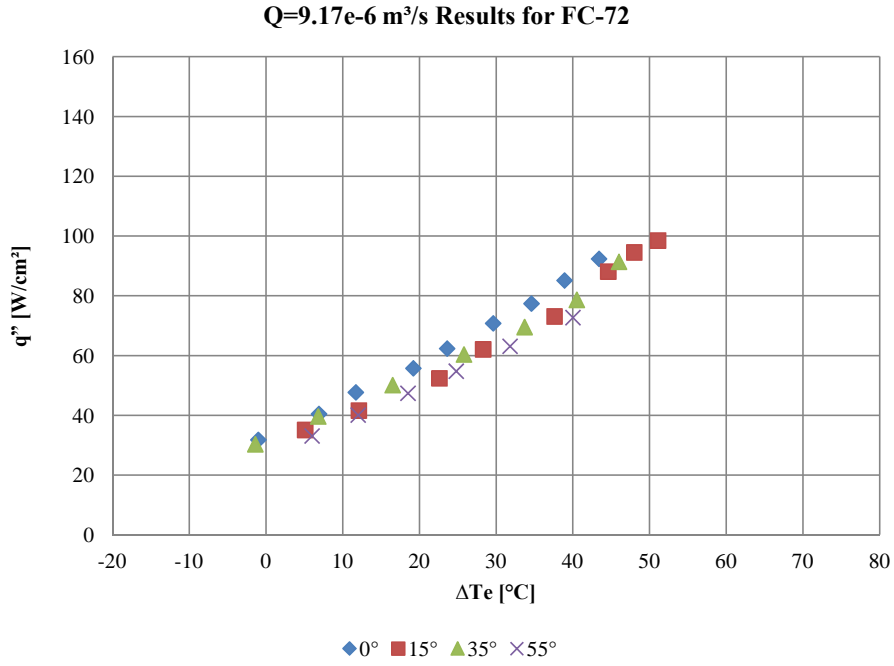


Figure 4.7: Boiling curves at different angles at $Q = 9.17 \times 10^{-6} \text{ m}^3/\text{s}$ for FC-72

There is an interesting phenomena in Figures 4.5, 4.6 and 4.7. Even angles are changed radically, boiling curves almost stay same except for spraying CHF points. It can be showed that, flow rate is the primary parameter determining heat transfer rate.

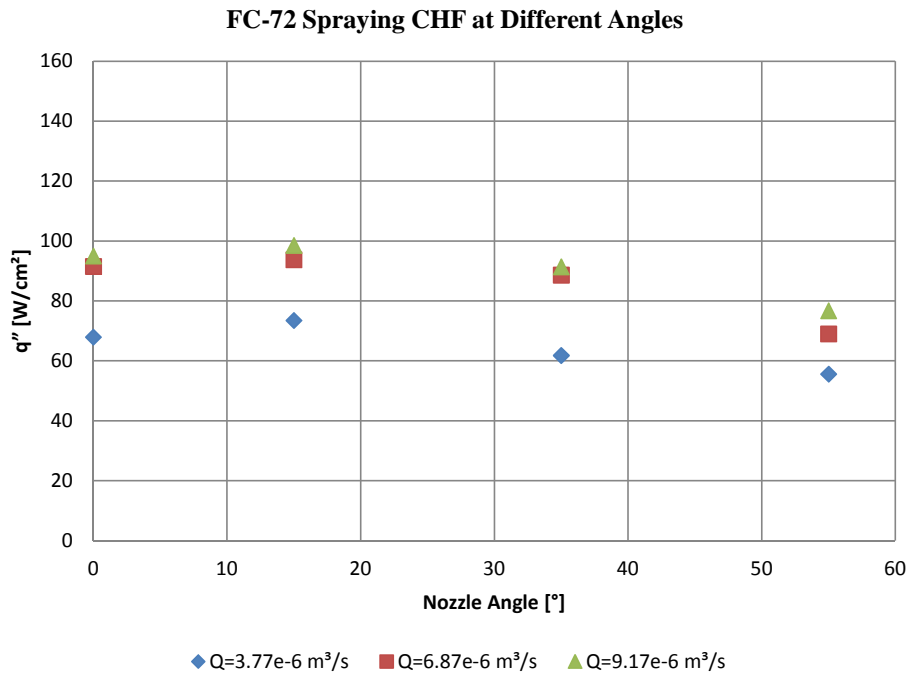


Figure 4.8: Spraying CHF values at different angles for FC-72

Figure 4.8 may be the most loaded figure containing almost all results belonged to FC-72. CHF for spraying stay about the same level up to 35°. Unluckily, it is observable drop when switching to 55°. The striking point of Figure 4.8, however, is that spraying CHF values are directly affected with breakup regime of the flow. It can be observed that, spraying CHFs are almost equal even flow rates are increased in second wind induced breakup regime.

4.2 FC-84 Results

As a first step, important dimensionless numbers' values for FC-84 experiments are given in Table 4.3. Bold pressure values stand for the operation points in the experiments.

Table 4.3: Dimensionless Numbers for FC-84 Experiments

ΔP [Bar]	Q [m^3/s]	Re_{d_0}	We_{d_0}	We_l	Oh
0.4	3.20E-06	15505	3	5425	1.20E-04
0.5	3.68E-06	17335	4	7187	1.20E-04
0.7	4.48E-06	20511	6	10648	1.20E-04
1.5	6.72E-06	30025	13	23899	1.20E-04
2	7.68E-06	34670	17	31273	1.20E-04
3	9.28E-06	42462	26	45654	1.20E-04

The breakup regime and surface contact regime conditions are expected as given in Table 2.1 and in Figure 2.3, respectively.

Table 4.4: Breakup and Contact Regimes for FC-84 Experiments

ΔP [Bar]	Q [m^3/s]	Breakup Regime	Contact Regime
0.4	3.20E-06	First wind induced	Prompt splash
0.5	3.68E-06	First wind induced	Prompt splash
0.7	4.48E-06	First wind induced	Prompt splash
1.5	6.72E-06	First wind induced	Prompt splash
2	7.68E-06	Second wind induced	Prompt splash
3	9.28E-06	Second wind induced	Prompt splash

0° Results for FC-84

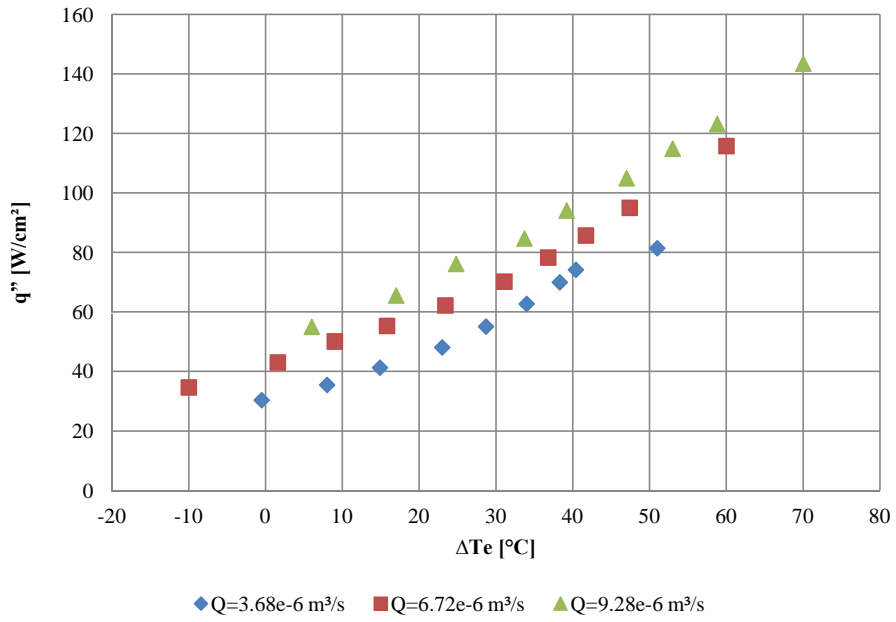


Figure 4.9: 0° boiling curve at different Q for FC-84

15° Results for FC-84

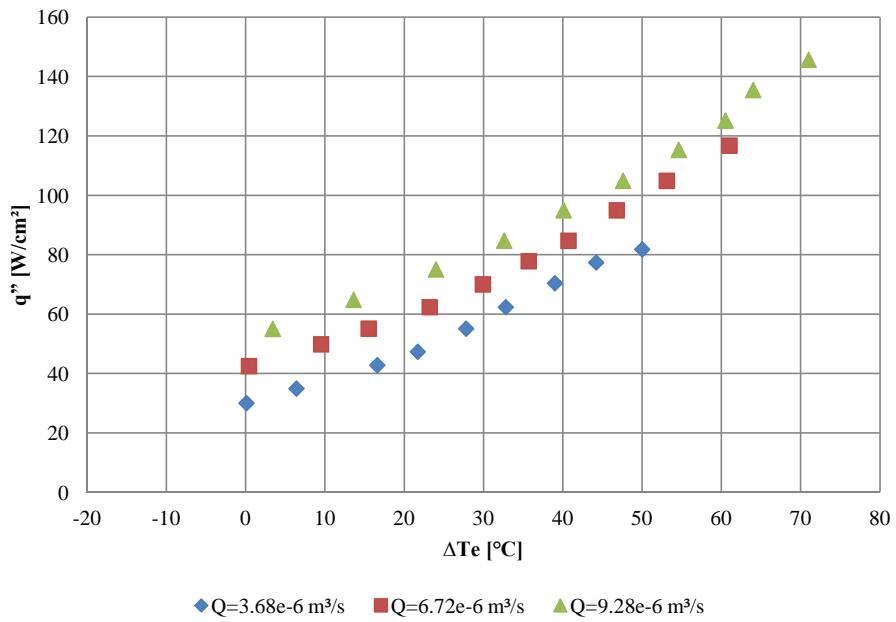


Figure 4.10: 15° boiling curve at different Q for FC-84

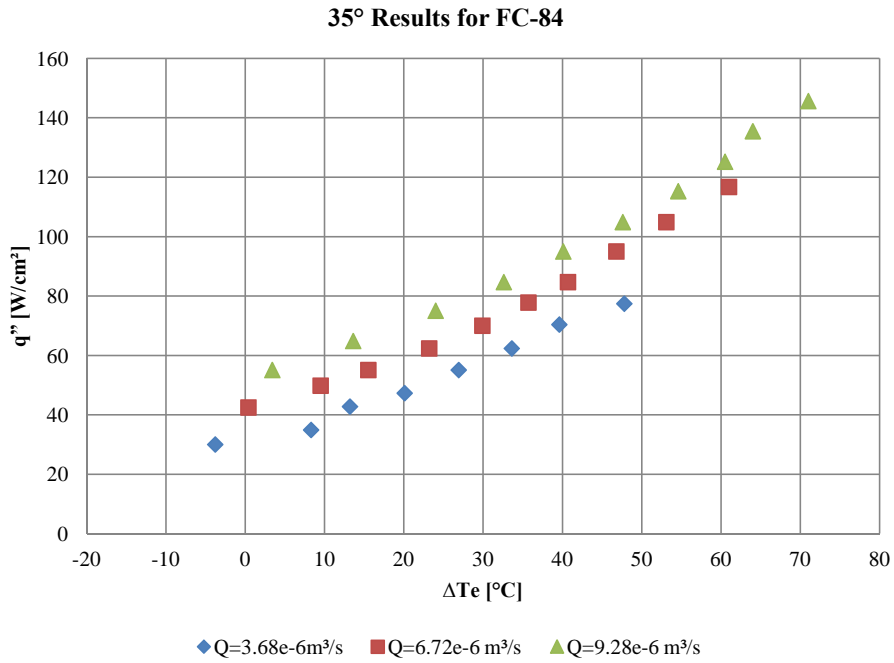


Figure 4.11: 35° boiling curve at different Q for FC-84

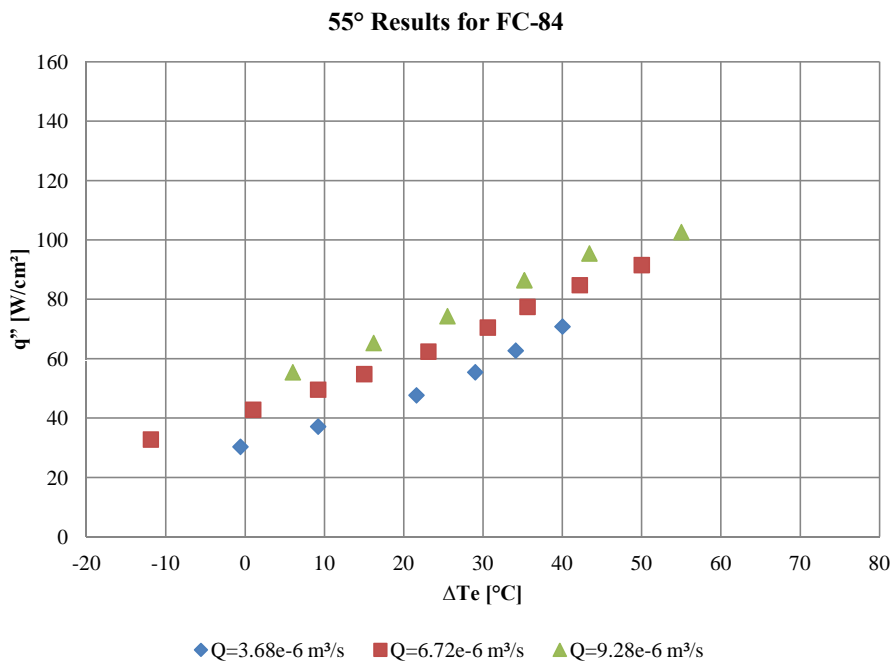


Figure 4.12: 55° boiling curve at different Q for FC-84

Similar results with FC-72 are also obtained for FC-84. Up to 35° boiling curves are almost same. Regime difference affects boiling curves in FC-84 results, too. In FC-84 measurements, first wind induced breakup regime is available for 0.5 Bar and 1.5 Bar measurements. Second

wind induced breakup regime is observed in 3 Bar measurements.

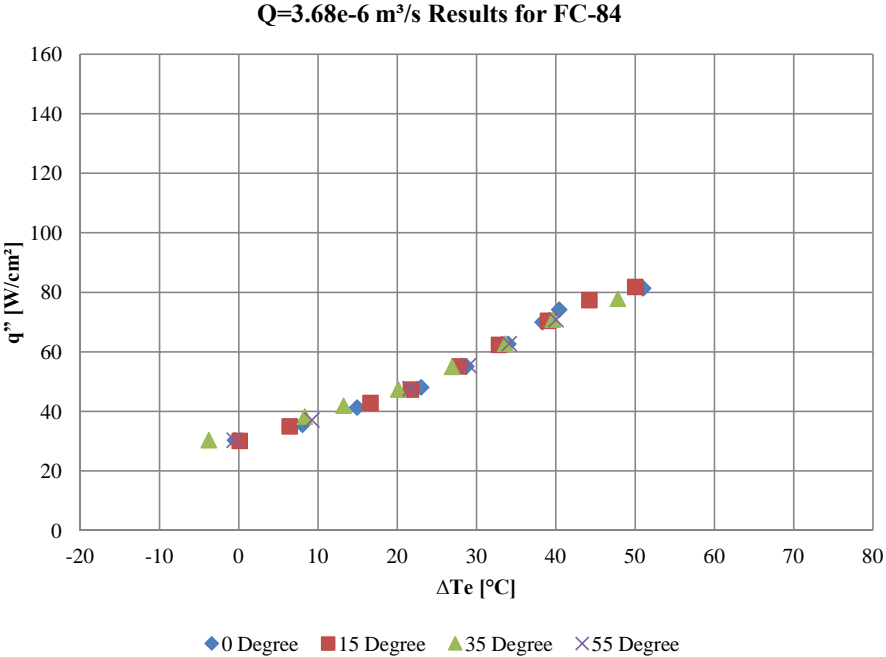


Figure 4.13: Boiling curves at different angles at $Q = 3.68 \times 10^{-6} \text{m}^3/\text{s}$ for FC-84

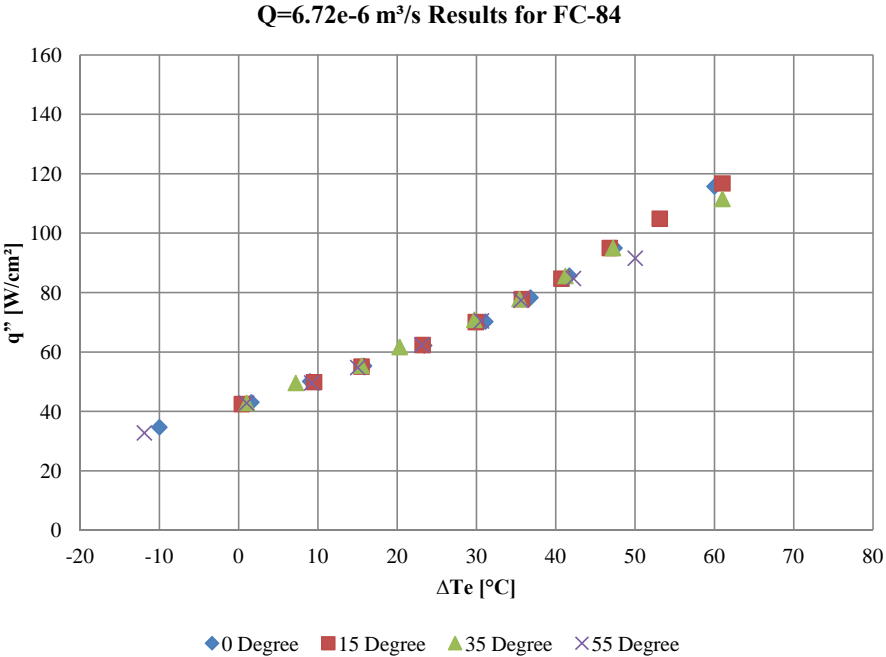


Figure 4.14: Boiling curves at different angles at $Q = 6.72 \times 10^{-6} \text{m}^3/\text{s}$ for FC-84

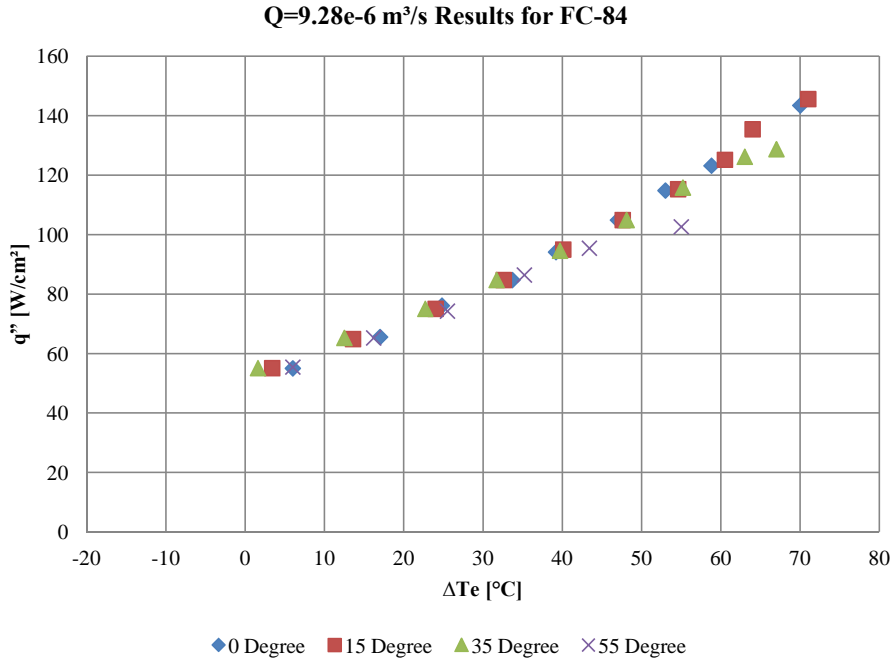


Figure 4.15: Boiling curves at different angles at $Q = 9.28 \times 10^{-6} \text{m}^3/\text{s}$ for FC-84

The relationship between angle and heat transfer performance act in the same way with FC-72 results. Angle do not affect boiling curves. The effect of angle is felt in spraying CHF values.

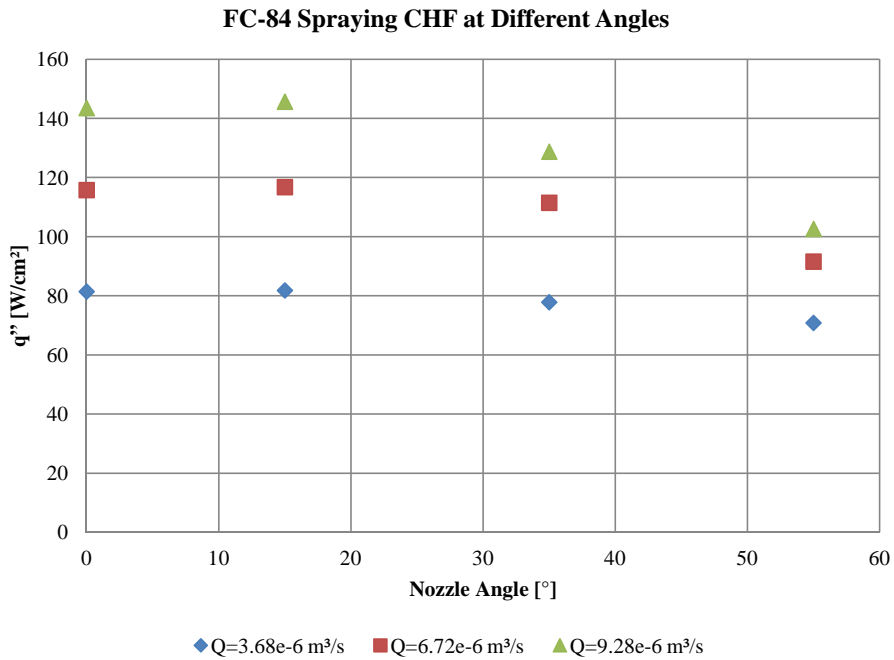


Figure 4.16: Spraying CHF values at different angles for FC-84

In Figure 4.16 spraying CHF values stay almost same until 35° but a gradual decrease is

available. Increasing flow rate also increases spraying CHF values. Nonetheless, the major difference between 4.8 and 4.16 is that similarity between uppermost two flow-rates spraying CHF values in FC-72 case are not present in FC-84 case. Since, the breakup regimes of two highest flow rates of FC-84 case are different.

4.3 Heat Loss Calculation

Images are taken from spraying chamber by thermal camera while spray cooling operation continues.



Figure 4.17: Thermal camera image from spraying chamber

When thermal camera images are carefully investigated, it is noted that the main heat loss is occurring at Teflon cylindrical insulation jacket. From the images, it can be clearly understood that other areas have almost zero thermal gradient. Therefore, major heat leakage is occurring around cylindrical area.

To calculate heat loss from cylindrical jacket, another thermal image is also captured. Besides, temperature values at inner and outer cylinder are measured.

1-D conduction is assumed for cylindrical jacket. Firstly, the jacket has full circle base area and heat loads are distributed symmetrically. Therefore, angle conduction is neglected. Secondly, temperature variation across the length of cylinder is not significant. For that reason, longitudinal conduction is also neglected. At the uppermost circular horizontal base of copper block has very small area. Horizontal plate natural convection from this area is also neglected. Only significant heat loss through the system is in radial direction from insulation jacket.

The radial direction heat loss is calculated by Equation 4.1 [13].

$$q_r = \frac{2\pi Lk(T_{s,1} - T_{s,2})}{\ln(r_2/r_1)} \quad (4.1)$$



Figure 4.18: Cylindrical insulation jacket thermal image

The length of the cylinder is 46mm . Inner radius is 16mm . Outer radius is 27.5mm . Conductivity of “Teflon” or PTFE material is 0.25 W/mK . The temperature measurements from thermal camera are $T_{s,2} = 33.2^\circ\text{C}$ and $T_{s,1} = 69.4^\circ\text{C}$. All in all, radial heat loss from insulation jacket is 4.83W .

The heat loss calculation above is carried out for 400W heat dissipation while using FC-84 fluid at 15° spraying angle with $6.72\text{e-}6\text{ m}^3/\text{s}$ flow rate.

4.4 Repeatability and Uncertainty of System

For calculation of repeatability of the system measurements, FC-72 at $Q = 6.87 \times 10^{-6}\text{ m}^3/\text{s}$ at 0° angle tests are carried out twice. Both experiments consist of 9 individual data points. In Table 4.5 these two experiment values are given.

Table 4.5: Two Same Experiments at $Q = 6.87 \times 10^{-6} \text{ m}^3/\text{s}$ by Using FC-72 at 0°

$q_1'' [\text{W}/\text{cm}^2]$	$T_1 [^\circ\text{C}]$	$q_2'' [\text{W}/\text{cm}^2]$	$T_2 [^\circ\text{C}]$
25.5	53.8	25.5	54.4
32.3	61.3	31.4	62.8
41.4	69.3	39.9	70.7
47.0	74.3	47.7	78
55.8	80	55.0	82.4
67.8	87	67.2	86.7
73.1	90.1	75.2	91
82.3	95.2	81.8	101
87.2	98.7	88.5	105.2

For calculation of repeatability following formulation is followed:

$$R_j = \left| \frac{M_{i+1,j} - M_{i,j}}{M_{i,j}} \right| \times 100 \quad (4.2)$$

Equation 4.2 supplies the percentage repeatability for j^{th} data point between the experiments $i + 1$ and i . To find average percentage repeatability Equation 4.3 is utilized.

$$\bar{R} = \sum_{j=1}^n \frac{R_j}{n} \quad (4.3)$$

The above procedure is applied for Table 4.5 and following average percentage repeatability values are obtained heat flux and temperature measurements respectively.

Table 4.6: Average Percentage Repeatability for Heat Flux and Temperature Measurements

\bar{R}_q	\bar{R}_T
1.69%	3.06%

As a last note, pressure transducer and mass flow meter have 1% and 0.1% relative percentage uncertainty values which are stated on their data sheets.

CHAPTER 5

DISCUSSION AND CONCLUSION

Experiments are completed and values are given in both tables and figures. The total experiment duration has exceeded 150 hours. In the experiments, any dangerous condition, such as fire, intoxication or component malfunction, have not been observed. Therefore, it can be said that experiments are successfully completed.

At the very start of the study, as mentioned at introduction chapter, it has been aimed to find a high performance cooling technique which can survive with electronics and demand low level supply. Spray cooling cannot be seen as a true address at first interpretation because, spraying applications are mostly carried out at metal production sites for quenching or cooling down hot extruded metals or burning fuels in internal combustion engines. The electronic cooling relation with spray cooling, on the other hand, has become available and more attractive since offering of micro level efficient atomizers and dielectric fluids in a commercial manner. Consequently, the power of two-phase heat transfer is multiplied with atomizers. Moreover, the boiling has been introduced to on top of critical electronic assemblies by using dielectric fluids.

After deciding over using spray for electronics cooling in any assembly, there are bunch of parameters to play for sustaining desired operation conditions. In this experiment, effects of spray angle, mass flow, pressure difference and fluid type to spraying performance are investigated. Before reaching experiment values, a closed loop spray cooling experiment setup is designed and produced.

At the experimental setup design and production stage, a careful and deep literature survey has been conducted. An open spray cooling setup is designed at the first design stage. Unluckily, 5 liters FC-72 have gone away to atmosphere after collecting 9 data. The fluids used in these experiments are far more expensive when compared to water or alcohol types. Therefore, loosing fluid to atmosphere through boiling cannot be tolerated. For that reason, a closed loop experiment setup is designed.

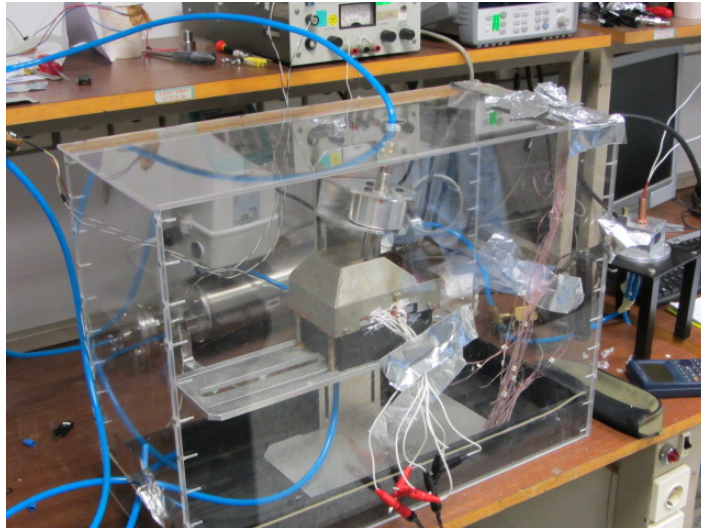


Figure 5.1: First design of experiment setup

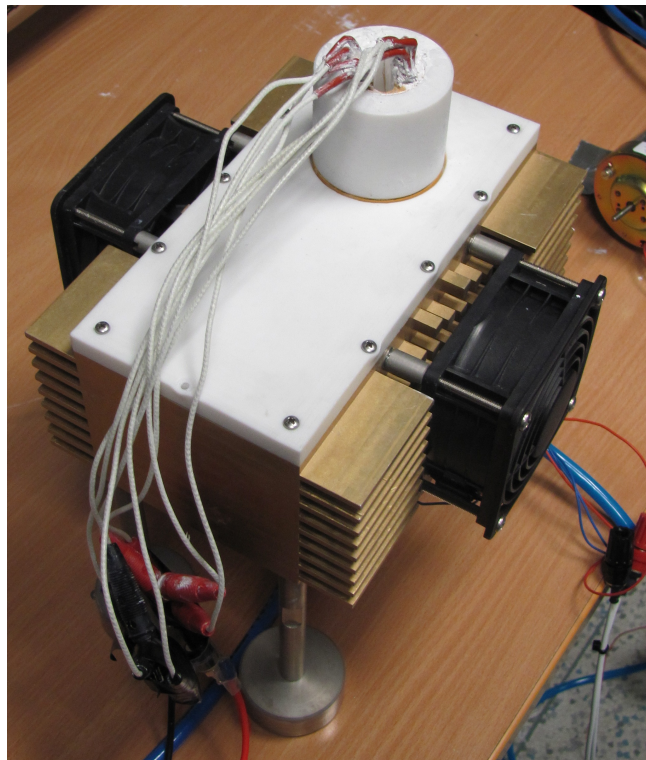


Figure 5.2: Last design of experiment setup

Experiment values are recorded for four different angles and three different pressure values by using two different fluids. At the data acquisition step, all the data has been stored by a mobile computer.

For last thing for this study the found values are compared with empirical models from the literature.

5.1 Discussion on Experimental Results

For both FC-72 and FC-84 results sections, firstly, boiling curves are drawn for increasing flow rate, Q , by keeping constant angle of nozzle. At the second set of FC-72 and FC-84 graphs, boiling curves for different angles at constant Q are drawn. As a last graph, spraying CHF variation with respect to nozzle angle for three different flow rates are presented.

- At the first set, it is observed that heat transfer coefficients are increased with flow rate. However, the increase in heat transfer is more drastic when contact regimes are transformed from first wind induced to second wind induced. Nevertheless, there is not much significant difference when contact and breakup regimes stay same. This effects can be seen at Figure 4.1, Figure 4.2, Figure 4.3 and Figure 4.4.
- At the second set of graphs, it can be said that heat transfer performances are almost same at same Q even angles are varied. These results can be seen at Figure 4.5, Figure 4.6 and Figure 4.7.
- For the last graph, 4.8, it can be seen that spraying CHF increases in a very small amount when switching 0° to 15° . 35° CHF values are almost same with 0° values. Nevertheless, 55° CHF values have dropped sharply when compared with other angles. This can be observed in Figure 4.8.

Same graphs are created for FC-84, too. FC-84 observations are:

- At first set of FC-84 experiment graphs, similar trends with FC-72 are obtained. It can be said that with increasing Q , heat transfer coefficients are increased. However, there is an interesting point in FC-84 experiments. The regime effects are observed again. For FC-72, experiments with the smallest flow rates are occurred on first wind induced breakup. On the other hand, for the two lowest flow rated FC-84 experiments, first wind induced breakup regime is available. Therefore, closeness of results of FC-72 has not been observed for FC-84 at the first set. The graphs of first set of FC-84 are Figure 4.9, Figure 4.10, Figure 4.11 and Figure 4.12.
- Angle has the same effect on boiling curves of FC-84 when compared to FC-72 results. These graphs are Figure 4.13, Figure 4.14 and Figure 4.15.
- For the CHF and angle relation of FC-84 can be seen at Figure 4.16. Similar trend is observed with FC-72. Nevertheless, this is the graph where regime effect is mostly sensed. When compared with Figure 4.8, it can be seen that results for the highest two Q experiment for FC-84 deviates more than FC-72 case.

All in all, for both experiments, it can be said that: If flow rate is increased for spray cooling applications, heat transfer performance is also increased. The angle of nozzle has little effect

for the angles 0°, 15° and 35° on heat transfer performance when compared to Q . However, spraying CHF has lost value when angle of nozzle is 55°. Nevertheless, most striking side of those experiments stays behind breakup regime classification. It is observed that results are mostly dependent on breakup and contact regime as it is explained previously.

5.2 Comparison of Experimental Results with Volumetric Flux Model (VFM)

Volumetric Flux Model (VFM) has been developed by Visaria et. al [18]. It is an empirical correlation for calculation of CHF at different angles and different volumetric fluxes. The derivation of VFM is placed in Appendix A.

After deriving a bunch of geometric correlation, most recent equation for determining CHF is [18]:

$$\frac{q''_{s,CHF}}{\rho_g h_{fg} \overline{Q}''} = 2.3 \left(\frac{\rho_f}{\rho_g} \right)^{0.3} \left(\frac{\rho_f \overline{Q}''^2 d_{32}}{\sigma} \right)^{-0.35} \left(1 + 0.0050 \frac{\rho_f C_{p,f} \Delta T_{sub}}{\rho_g h_{fg}} \right) \left(\frac{f_1^{0.30}}{f_2} \right) \quad (5.1)$$

Experimental results and VFM results are compared:

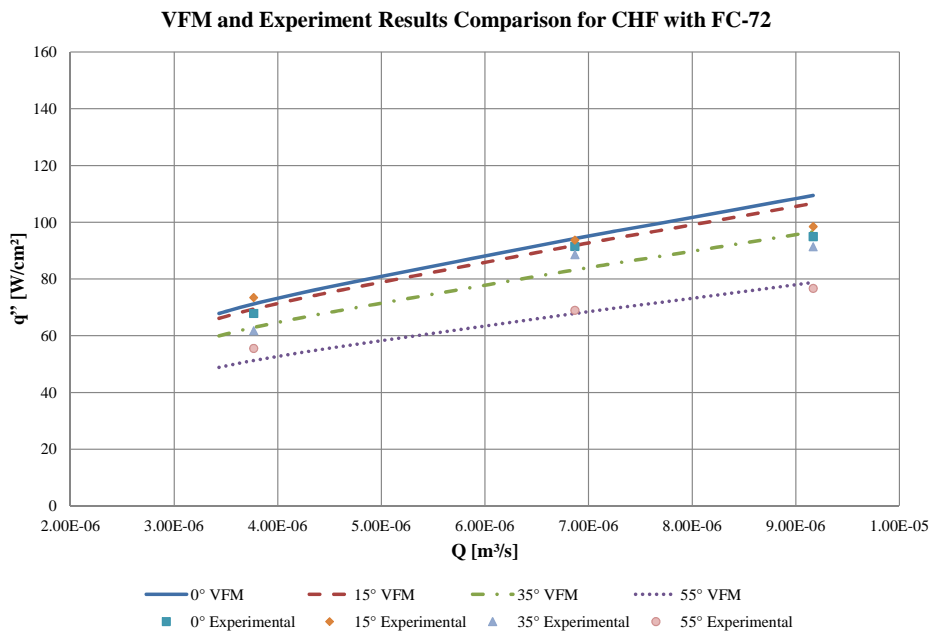
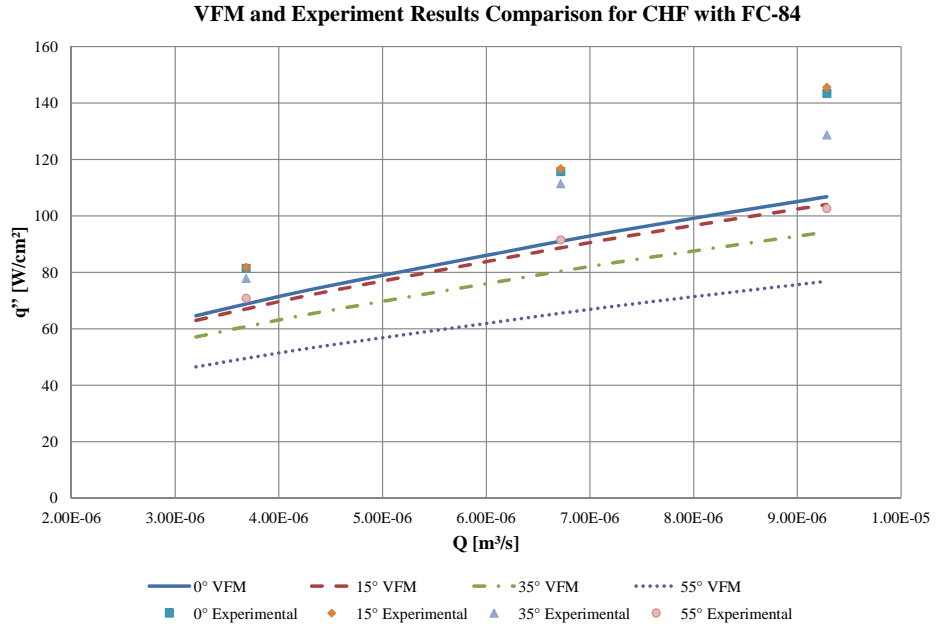


Figure 5.3: VFM and experimental results comparison for FC-72



For both of the experiments general trends have matched with each other. However, there is more deviation for FC-84 case when compared to FC-72 case. The tabulated data for these comparisons are given in Table 5.1 and Table 5.2 for FC-72 and FC-84, respectively.

Table 5.1: Comparison of Experimental and Empirical Spraying CHF for FC-72

Angle of nozzle	Spraying CHF FOR FC-72 [W/cm^2]					
	EXPERIMENTAL			VFM		
	Qx10e-6 [m^3/s]					
	3.77	6.87	9.17	3.77	6.87	9.17
0°	68	92	95	71	94	109
15°	73	94	99	69	92	107
35°	62	89	91	63	83	97
55°	56	69	77	51	68	79

Table 5.2: Comparison of Experimental and Empirical Spraying CHF for FC-84

Angle of nozzle	Spraying CHF FOR FC-84 [W/cm^2]					
	EXPERIMENTAL			VFM		
	Qx10e-6 [m^3/s]					
	3.68	6.72	9.28	3.68	6.72	9.28
0°	81	116	143	69	91	107
15°	82	117	146	67	89	104
35°	78	111	129	61	80	94
55°	71	92	103	50	66	77

The possible reason behind the almost perfect match of FC-72 data with empirical correlation is that VFM relation is developed by after many spray cooling experiments using FC-72. Visaira et. al [21] have used same nozzle used in this current study with the flow rate interval of $3.5 - 3.86 \times 10^{-6} \text{m}^3/\text{s}$. Besides, subcooling of VFM experiments consist of same subcooling degree in this experiment. Therefore, VFM correlation for FC-72 works perfect. On the other side, FC-84 results are far more separated from VFM prediction curves. Nevertheless, FC-84 results carry the same character with VFM results with a constant shift to upper heat flux side.

5.3 Conclusion

1. The main parameter folded heat transfer rate is increasing flow rate. In other words, if the pressure supplied to the nozzle is increased, more heat can be transferred from heated area. This is because of droplet size which is broken into more smaller size with increasing momentum. As a result, the smaller droplets are created, the larger heat transfer coefficients are available.
2. Breakup process play a crucial role in heat transfer regime of a spray cooled system. When results are investigated, it can be clearly interpreted that heat transfer rates of different breakup regimes are radically separated from each other. For that reason, just increasing of supplied pressure to the nozzle may not show the superior effect of breakup regime alteration. In conclusion, boiling can be more efficient as it is getting closer to atomization side.
3. Changing angle has an interesting effect on spray cooling. Up to a certain value of angle boiling curves and even spraying CHF values are very similar to each other. However, spraying CHF drops significantly beyond a critical angle. Nevertheless, boiling curves at different angles with same flow rates are almost same except for their spraying CHF values. Consequently, a nozzle operation angle can be chosen near the critical angle for the sake of smaller electronic packages since, same heat transfer performance can be obtained.
4. The possible reason in deviation of FC-84 data with VFM correlation is the poor prediction of subcooling effect. The weakest side of VFM equation is prediction of subcooling because, Visaira et. al [18] have modified former VFM equation for better prediction of subcooling. For the FC-84 case, VFM equation can be modified for better match. Unluckily, the coefficient of subcooling effect in VFM equation may not be a constant. It can carry a nonlinear behavior or its value can be changed for different fluids.

5.4 Future Work

Current study can be enhanced in many aspects. Firstly, Equation 5.1 can be developed for different fluids and subcooling ranges. Another crucial study may be a CFD analysis for a

single droplet for different surface patterns, angles, roughness etc. Then those analyzes can be verified by real data which can be obtained by special visualization techniques. Besides, obtained data can be converted into an empirical equation. Multiple nozzle behavior and optimization of a multiple nozzle field are another suggested works.

REFERENCES

- [1] <http://commons.wikimedia.org/wiki/File:Eniac.jpg>.
- [2] <https://tr.m.wikipedia.org/wiki/Dosya:C64system.jpg>.
- [3] <http://www.digitallifeplus.com/317/20120117amd-ultrabook-prices/>.
- [4] Gordon E. Moore. Cramming more components onto integrated circuits. *Electronics*, 38, 1965.
- [5] <http://www.flickr.com/photos/linuxtuxguy/4387996904/>.
- [6] Arthur H.Lefebvre. *Atomization and Sprays*. Taylor&Francis, Boca Raton, 1989.
- [7] Huimin Liu. *Science and Engineering of Droplets*. Noyes Publications/ William Andrew Publishing, Norwich, 1999.
- [8] G.G. Nasr, A.J. Yule, and L.Bendig. *Industrial Sprays and Atomization*. Springer, Wiltshire, 2002.
- [9] John D. Bernardin, Clinton J. Stebbins, and Issam Mudawar. Effect of surface roughness on water droplet impact history and heat transfer regimes. *Int. J. Heat and Mass Transfer*, 40(1):73–88, 1997.
- [10] Eric A. Silk, Jungho Kim, and Ken Kiger. Enhanced Surface Spray Cooling With Embedded and Compound Extended Surface Structures. *IEEE*, 6:215–223, 2006.
- [11] L. Bayvel and Z. Orzechowski. *Liquid Atomization*. Taylor&Francis, Washington, 1993.
- [12] K. Barth, N. Delruelle, A. Dudarev, G. Passardi, R. Pengo, M. Pezzetti, O. Pirotte, H. T. Kate, E. Baynham, and C. Mayri. First Cool-Down and Test at 4.5 K of the ATLAS Superconducting Barrel Toroid Assembled in the LHC Experimental Cavern. *IEEE Transactions on Applied Superconductivity*, 18:383–386, 2008.
- [13] Incropera, DeWitt, Bergman, and Lavine. *Fundamentals of Heat and Mass Transfer*. John Wiley&Sons, 2007.
- [14] Shiro Nukiyama. The maximum and minimum values of the heat Q transmitted from metal to boiling water under atmospheric pressure. *International Journal of Heat and Mass Transfer*, 9(12):1419–1433, 1966.
- [15] S. S. Kutateladze. On the Transition to Film Boiling under Natural Convection. *Kotlobostroenie*, (3):10–12, 1948.
- [16] N. Zuber. Hydrodynamic Aspects of Boiling Heat Transfer. *ASME*, (80):711, 1958.

- [17] Satish G. Kandlikar. A Theoretical Model to Predict Pool Boiling CHF Incorporating Effects of Contact Angle and Orientation. *Journal of Heat Transfer*, 123:1071–1079, 2001.
- [18] Milan Visaria and Issam Mudawar. Application of Two-Phase Spray Cooling for Thermal Management of Electronic Devices. *IEEE Transactions on Components and Packaging Technologies*, 34(4):784–793, 2009.
- [19] L. Ortiz and J. E. Gonzalez. Experiments on Steady State High Heat Fluxes Using Spray Cooling. *Experimental Heat Transfer: A Journal of Thermal Energy Generation, Transport, Storage, and Conversion*, 12:215–233, 1999.
- [20] W. Jia and H.-H. Qiu. Experimental investigation of droplet dynamics and heat transfer in spray cooling. *Experimental Thermal and Fluid Science*, 27:829–838, 2003.
- [21] Milan Visaria and Issam Mudawar. Theoretical and experimental study of the effects of spray inclination on two-phase spray cooling and critical heat flux. *International Journal of Heat and Mass Transfer*, 51:2398–2410, 2008.
- [22] T. Deiters and I. Mudawar. Optimization of Spray Quenching for Aluminum Extrusion, Forging, or Continuous Casting. *J. Heat Treating*, 1:9–18, 1989.
- [23] A. C. Cotler, E. R. Brown, V. Dhir, and M. C. Shaw. Chip-Level Spray Cooling of an LD-MOSFET RF Power Amplifier. *IEEE Transactions on Components and Packaging Technologies*, 2(27):411–416, 2004.
- [24] R. G. Mertens, L. Chow, K. B. Sundaram, R. B. Cregger, D. P. Rini, L. Turek, and B. A. Saarloos. Spray Cooling of IGBT Devices. *Transactions of the ASME*, 129:316–323, 2007.
- [25] I. Mudawar, D. Bharathan, K. Kelly, and S. Narumanchi. Two-Phase Spray Cooling of Hybrid Vehicle Electronics. In *Itherm*, 2008.
- [26] B. Horacek, J. Kim, and K. T. Kiger. Spray Cooling Using Multiple Nozzles: Visualization and Wall Heat Transfer Measurements. *IEEE Transactions on Device and Materials Reliability*, 4:614–625, 2004.
- [27] C. R. Orloff and M. Vogel. Spray Cooling Heat Transfer -Test and CFD Analysis. In *27th IEEE SEMI-THERM Symposium*, 2011.
- [28] J. D. Bernardin, C. J. Stebbins, and I. Mudawar. Effects of surface roughness on water droplet impact history and heat transfer regimes. *International Journal of Heat and Mass Transfer*, 40:73–88, 1996.
- [29] M. Visaria and I. Mudawar. A Systematic Approach to Predicting Critical Heat Flux for Inclined Sprays. *ASME-Journal of Electronic Packaging*, 129:452–459, 2007.
- [30] M. Visaria and I. Mudawar. Effects of high subcooling on two-phase spray cooling and critical heat flux. *International Journal of Heat and Mass Transfer*, 51:5269–5278, 2008.
- [31] M. S. El-Genk and J. L. Parker. Nucleate boiling of FC-72 and HFE-7100 on porous graphite at different orientations and liquid subcooling. *Energy conversion and management*, 49:733–750, 2008.

- [32] A. Pautsch and T. Shedd. Spray impingement cooling with single- and multiple-nozzle arrays. Part I: Heat transfer data using FC-72. *International Journal of Heat and Mass Transfer*, 48:3167–3175, 2005.
- [33] M. Fabbri and V. K. Dhir. Optimized Heat Transfer for High Power Electronic Cooling Using Arrays of Microjets. *ASME*, 127:760–769, 2005.
- [34] A. Moreira and M. Panao. Heat transfer at multiple-intermittent impacts of a hollow cone spray. *International Journal of Heat and Mass Transfer*, 49:4132–4151, 2006.
- [35] W. Deng and A. Gomez. Electrospray cooling for microelectronics. *International Journal of Heat and Mass Transfer*, 54:2270–2275, 2011.
- [36] C. E. Bash, C. D. Patel, and R. K. Sharma. Inkjet Assisted Spray Cooling of Electronics. In *Proceedings of IPACK03*, 2003.
- [37] K. Yoshida, Y. Abe, T. Oka, Y. Mori, and A. Nagashima. Spray cooling under reduced gravity conditions. *Journal of Heat Transfer*, 123:309–318, 2001.
- [38] Jungho Kim. Spray cooling heat transfer: The state of the art. *International Journal of Heat and Fluid Flow*, 28:753–767, 2007.
- [39] K. A. Estes and I. Mudawar. Correlation of Sauter mean diameter and critical heat flux for spray cooling of small surfaces. *International Journal of Heat and Mass Transfer*, 38:2985–2966, 1995.

APPENDIX A

DERIVATION OF VFM

The all derivations in Appendix A are carried out by Visaria et. al [18]

As a first step nomenclature for inclined spray is given in A.1.

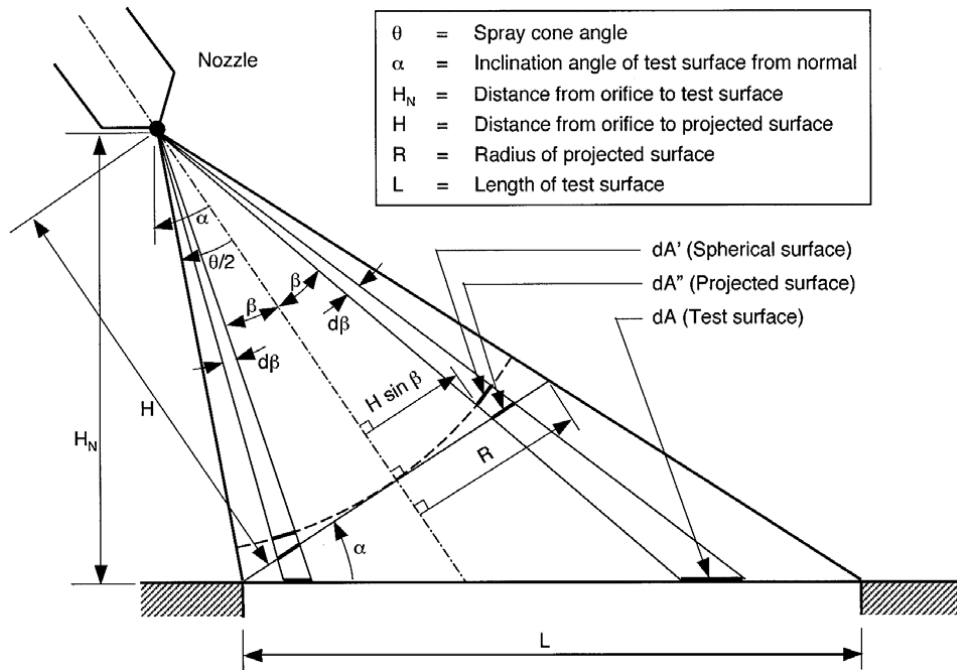


Figure A.1: Nomenclature for inclined spray

The projection distance H is found by following equation:

$$H = \frac{L}{2} [\cos \alpha \cot(\theta/2) - \sin \alpha] \quad (\text{A.1})$$

Then SMD is found.

$$\frac{d_{32}}{d_0} = 3.67 [We_{d_0}^{1/2} Re_{d_0}]^{-0.259} \quad (\text{A.2})$$

Where;

$$Re_{d_0} = \frac{\rho_f(2\Delta P/\rho_f)^{1/2}d_0}{\mu_f} \quad (A.3)$$

$$We_{d_0} = \frac{\rho_a(2\Delta P/\rho_f)d_0}{\sigma_f} \quad (A.4)$$

To find average volumetric flux:

$$\bar{Q}'' = \frac{Q}{\frac{\pi}{4}L^2 \cos \alpha \sqrt{1 - \tan^2 \alpha \tan^2(\theta/2)}} \quad (A.5)$$

Then to find the other geometric factors, differential area ratio graph is offered. In Figure A.2 Nozzle 1 is the same nozzle used in current study.

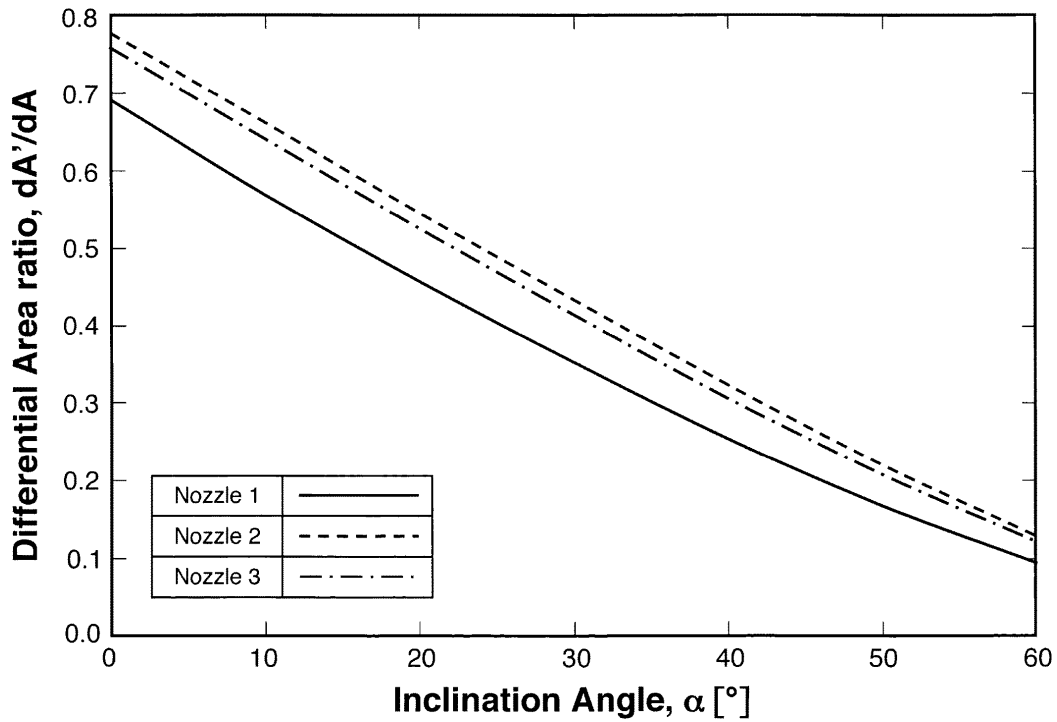


Figure A.2: Differential area ratio with respect to inclination angle, dA'/dA

Then the geometric factors are found:

$$f_1 = \frac{1}{8} \left(\frac{L}{H} \right)^2 \frac{\cos \alpha \sqrt{1 - \tan^2 \alpha \tan^2(\theta/2)}}{1 - \cos(\theta/2)} \frac{dA'}{dA} \quad (A.6)$$

$$f_2 = \frac{1}{\left[\frac{\pi}{4} \cos \alpha \sqrt{1 - \tan^2 \alpha \tan^2(\theta/2)} \right]} \quad (\text{A.7})$$

By using all equations above:

$$\frac{q''_{s,CHF}}{\rho_g h_{fg} \overline{Q}''} = 2.3 \left(\frac{\rho_f}{\rho_g} \right)^{0.3} \left(\frac{\rho_f \overline{Q}''^2 d_{32}}{\sigma} \right)^{-0.35} \left(1 + 0.0050 \frac{\rho_f C_{p,f} \Delta T_{sub}}{\rho_g h_{fg}} \right) \left(\frac{f_1^{0.30}}{f_2} \right) \quad (\text{A.8})$$